Neurophysiological effects of simulated auditory prosthesis stimulation

Final Report

Neural Prosthesis Program
Contract N01-DC-9-2107

October 2003

P.J. Abbas, C.A. Miller, J.T. Rubinstein, B.K. Robinson, H. Mino, N. Hu, K.V. Nourski, F.C. Jeng, C.L. Runge Samuelson

Department of Otolaryngology-Head and Neck Surgery
&
Department of Speech Pathology and Audiology

University of Iowa

Iowa City, Iowa, USA

File: N01-DC-9-2107QPRFF.PDF

Neurophysiological effects of simulated auditory prosthesis stimulation

Neural Prosthesis Program

NIH Contract N01-DC-9-2107

Final Report

TABLE OF CONTENTS

I. Introduction

The purpose of the work performed under contract N01-DC-9-2107 was to explore issues involving the transfer of information from implantable auditory prostheses to the central nervous system. Our research conducted over the past four-year period has employed physiologic measures and computational models to investigate fundamental properties of electric stimulation of the auditory nerve. Original efforts conducted under the previous contract (N01-DC-6-2111) employed simple electrical stimuli (e.g., single monophasic pulses delivered by a monopole) in order to characterize fundamental response properties and provide baseline measures to develop realistic computational models of neural responses. In the present contract period, we expanded those efforts to more complex stimuli. By combining experimental measures of those response properties with improved model simulation, we proposed to provide a better understanding of the physiologic basis of those responses and facilitate the development of novel stimulation strategies for improved information transfer.

This report outlines the work done under this contract. In several areas we have summarized data from our previous contract that were relevant to the goals and results from the present contract period. In areas where we have previously reported results in quarterly progress reports, we have referred to those reports and/or publications. Those progress reports and publications provide more details of both methods and experimental results relative to each topic. Finally, we have attempted to identify specific applications of the work, both stimulation and recording paradigms, where results have been applied to clinical populations.

A feature of this work was the effort to coordinate measures of the evoked compound action potential measures (ECAP) with single-fiber measures to provide more accurate interpretations of the former. We used both guinea pigs and cats to record the ECAP and cats for single auditory nerve fiber measures. The details of those recording methods are presented in previous publications (Miller et al., 1998; Miller et al., 1999a). Note that, unless specifically noted, the animal data reported here were obtained from cochleae that were acutely deafened with an aminoglycoside drug to provide a model of the deafened auditory system.

II. Responses to monopolar, monophasic stimuli

ECAP and single-fiber responses (Contract N01-DC-6-2111)

A goal of our first contract was to characterize responses of the peripheral auditory system to 40 μs monophasic, monopolar stimulation. Using acutely deafened cat and guinea pig models, we characterized ECAP responses across a range of stimulus amplitudes, polarities, and durations (Miller et al., 1998). Response measures included latency, morphology, amplitude, growth rate, and an estimate of conduction velocity. The results revealed several differences between cathodic and anodic responses that are often obscured with biphasic stimuli (Miller et al., 2001c), suggesting that monophasic, monopolar stimuli are needed for unambiguous assessment of polarity effects and issues related to excitation mechanisms. Significant inter-species differences were also found, underscoring the likely impact of anatomical differences on the response of the peripheral auditory system.

Using the same stimulus protocols, single-fiber responses were obtained for a 257 feline fibers (Miller et al., 1999a). Several response characteristics were analyzed, including threshold, mean latency, jitter (standard deviation of spike latency), and relative spread. Relative spread (RS) – the normalized standard deviation of an integrated gaussian fit to the I/O function (Verveen, 1961) – is a measure proportional to the fiber's dynamic range. These fiber properties proved useful in assessing the accuracy of our biophysical computational models. Also, the use of basic (monophasic, monopolar) stimuli clarified some site-of-excitation issues that had been unresolved in the literature. Detailed quantitative analyses of RS, jitter, and latency (Miller et al., 1999b) were consistent with a hypothesis that a minority of fibers (i.e., fibers with closest passage to the stimulating electrode) was activated at membrane sites peripheral to the cell body. We concluded that, for a monopolar stimulus field produced by an electrode placed in the base of the scala tympani, most fibers are activated central to the cell body, with the cathodic site more peripheral than the anodic site.

Model of ECAP generation

These properties of single fibers were incorporated into an integrative model to predict the response waveform and amplitude growth of the ECAP (Miller et al, 1999b). The model uses several characteristics of the single fiber responses: threshold distribution, fiber latencies, fiber jitter, and response growth (i.e., relative spread). Model results showed a good approximation to experimental ECAP characteristics but also established that the most important factor in determining the form of ECAP growth is the fiber threshold distribution. We interpret those results to suggest that measures of ECAP amplitude can be applied to estimate the number of active fibers, at least under the stimulus conditions investigated. In this contract period, we performed additional experiments, described in Section VII that provided additional insight into the interpretation of this evoked potential.

Spatial effects on temporal properties of electrical stimulation (QPR7)

One of the goals of this contact sought to further develop a realistic model of auditory nerve fiber activation with electrical stimulation. Several modifications of the Rubinstein (1995) model were developed and evaluated over the period of this contract (Matsuoka et al., 2001; Mino et al 2002, Rubinstein and Santina, 2002).

Although analytical and computational models suggest some interaction between spatial properties of the stimulus field and temporal properties of neuronal response (Rubinstein, 1988), we previously considered those effects to be of secondary importance to understanding stimulus-response relationships between a stimulus field and a single modeled fiber. Despite significant efforts, our model simulations had previously failed to account for the 50-100 μs spike jitter (assessed at 50% firing efficiency) observed in our animal models. Despite the ability of the model to account for most fundamental response properties (i.e., threshold distribution, anodal/cathodal threshold ratios, latency differences in cat, relative spread, integrative time constant, refractory period and refractory effects on spike amplitude and latency), no model parameter manipulation was previously able to produce spike jitter greater than 40-50 μs. In this contract period, we determined that manipulation of electrode-fiber distance has a profound effect on spike jitter (Figure 1, Mino et al., in press). This occurs due to the fact that a more distant electrode recruits more nodes of Ranvier in the spike initiation process. However, to maintain a constant FE, each contributing node fires at a lower FE. As is clear from both models and single-unit studies, lower FE stimuli evoke higher jitter. This unexpected effect corrected one of the remaining deficiencies of the model in simulating single-fiber and ECAP responses and demonstrated that temporal response characteristics can be profoundly affected by manipulation of the spatial properties of the electric field.

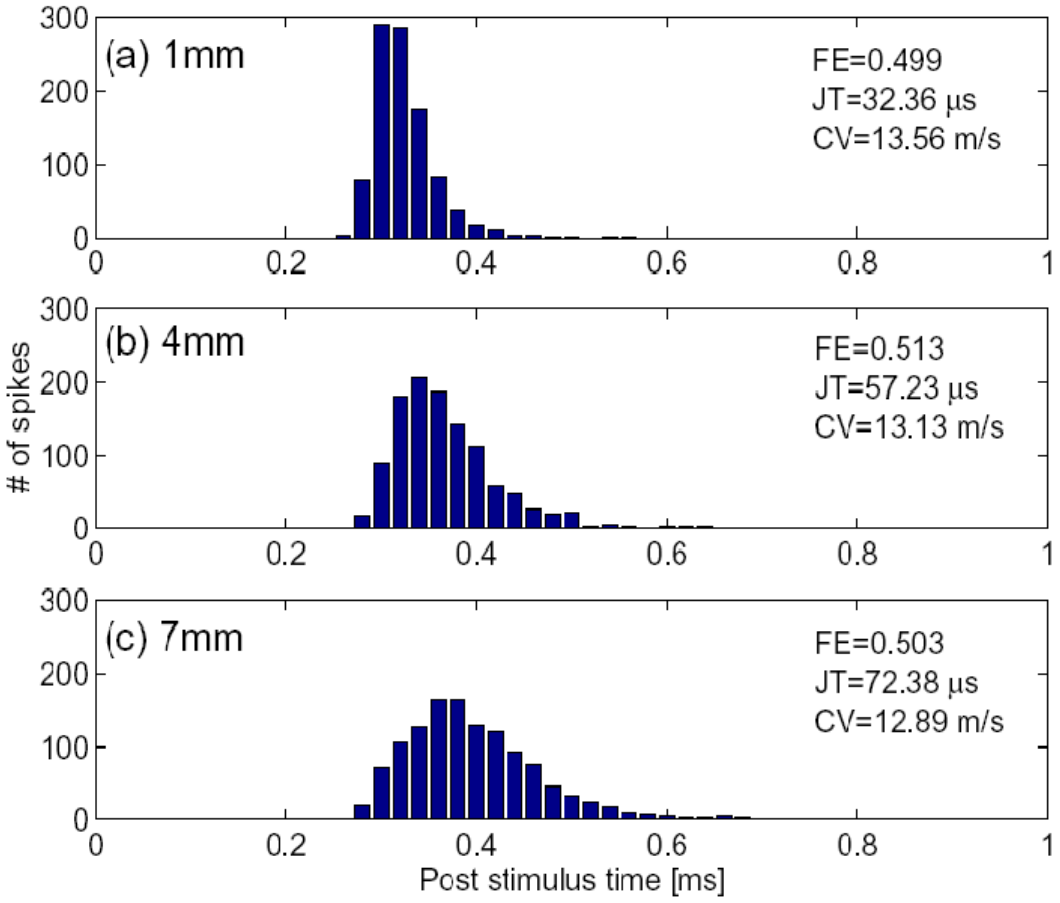

Figure 1 PST histograms generated by a biophysical computation model to investigate the effects of electrode-to-fiber distance. Histograms were produced from the spike times in response to 500 identical stimulus pulses at the electrode-to-fiber distances of 1 mm, 4 mm and 7mm. The estimated firing efficiency (FE), jitter (JT) and conduction velocity (CV) are shown in the inset.

III. Responses to biphasic and pseudomonophasic stimuli

ECAP and single fiber data (QPR2)

While monophasic stimuli are well suited for assessing excitation mechanisms, they fundamentally differ from the biphasic stimuli typically used by prosthetic devices. To bridge this gap, we conducted within-animal ECAP and within-fiber comparisons of the responses to monophasic, biphasic, and "pseudomonophasic" stimuli (the term "pseudomonophasic" typically refers to a biphasic pulse in which the second phase duration is much greater than the first). For all three stimuli, the duration of the first phase was fixed at 40 μs. ECAP responses were again collected from cats and guinea pigs to characterize threshold, maximum growth rate, and maximum amplitude. Figure 2 provides comparisons of response properties to monophasic and biphasic stimuli for both individual subjects (open symbols) as well as mean values (filled symbols) for each species. As in our analysis of monophasic stimuli, some across-species differences were observed (Figure 2) and are discussed in detail elsewhere (Miller et al., 2001c).

ECAP biphasic-vs.-monophasic comparisons were augmented by single-fiber studies that employed identical stimulus protocols. Figure 3 summarizes how fundamental properties (threshold, mean latency, jitter, and RS) differ for the two stimuli. Individual single-fiber data are plotted with open circles; filled symbols indicate mean values. Significant group differences were observed in threshold and spike latency (Figure 3 A, B). We also found a significant bias toward higher RS values with monophasic pulses, indicating that the shape of the stimulus waveform influences fiber dynamic range. As discussed in Miller et al., (2001c), the ECAP and single-fiber data also indicate that nerve-fiber recruitment and possibly sites of initiation are strongly influenced by the waveform shape. Finally, this study analyzed the effectiveness of pseudomonophasic stimuli in reducing ECAP and single-fiber thresholds. Second-durations as low as 500 μs resulted in thresholds similar to that of monophasic stimuli (Miller et al., 2001c).

Model results (QPR3)

The experimental data with biphasic stimulation was analyzed in the context of the biophysical model (Rubinstein et al., 2001). A statistically significant relationship between monophasic/biphasic threshold ratios and monophasic-biphasic latency differences was found that is consistent with both modes of stimulation occurring at the same "cathodal site" for cathodal monophasic and cathodal-first biphasic stimulation. The relationship also suggests that current integration at the "cathodal site" is solely responsible for both latency and threshold differences. Computational simulations were consistent with this hypothesis and also accounted for the different monophasic/biphasic threshold ratio obtained by Shepherd & Javel (1999). The difference was determined to be due to the longer pulse width used by these investigators (Figure 3-16, Rubinstein et al., 2001).

IV. Refractory properties of auditory nerve fibers

Refractory properties of single nerve fibers (QPR5)

While the above studies defined basic response properties, subsequent work was performed to assess fiber responses to repetitive electric stimuli. Single-fiber refractory properties were assessed using a forward-masking paradigm consisting of a probe pulse preceded by a masking pulse. Both the masker and probe were monophasic pulses of the same polarity separated by a masker-probe interval (MPI). Responses to masked probe stimuli were assessed at several probe levels and MPI values. An extensive assessment of

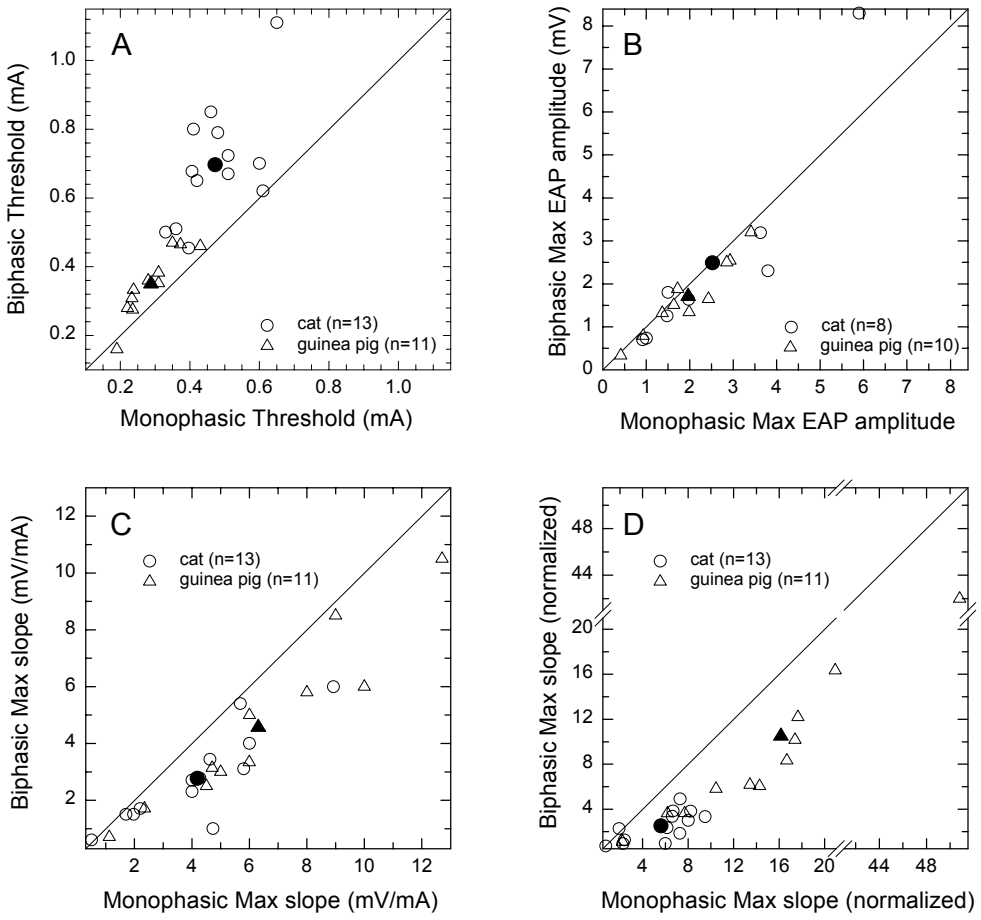

Figure 2 Summary of ECAP measures obtained from 13 cats and 11 guinea pigs, with each graph presenting a comparison of measures obtained with monopolar and bipolar intracochlear stimulation. Panel A: Threshold, defined as the stimulus level producing an amplitude 10% of the maximum amplitude. Panel B: Maximum ECAP amplitude achieved for each animal. Panel C: Maximum slope of each subject's amplitude-vs-level function. Data were computed as the maximum rate-of-increase over all the segments of each amplitude-level function. Panel D: Maximum slope data (similar to that of panel C), normalized to account for differences in thresholds produced by monophasic and biphasic stimuli.

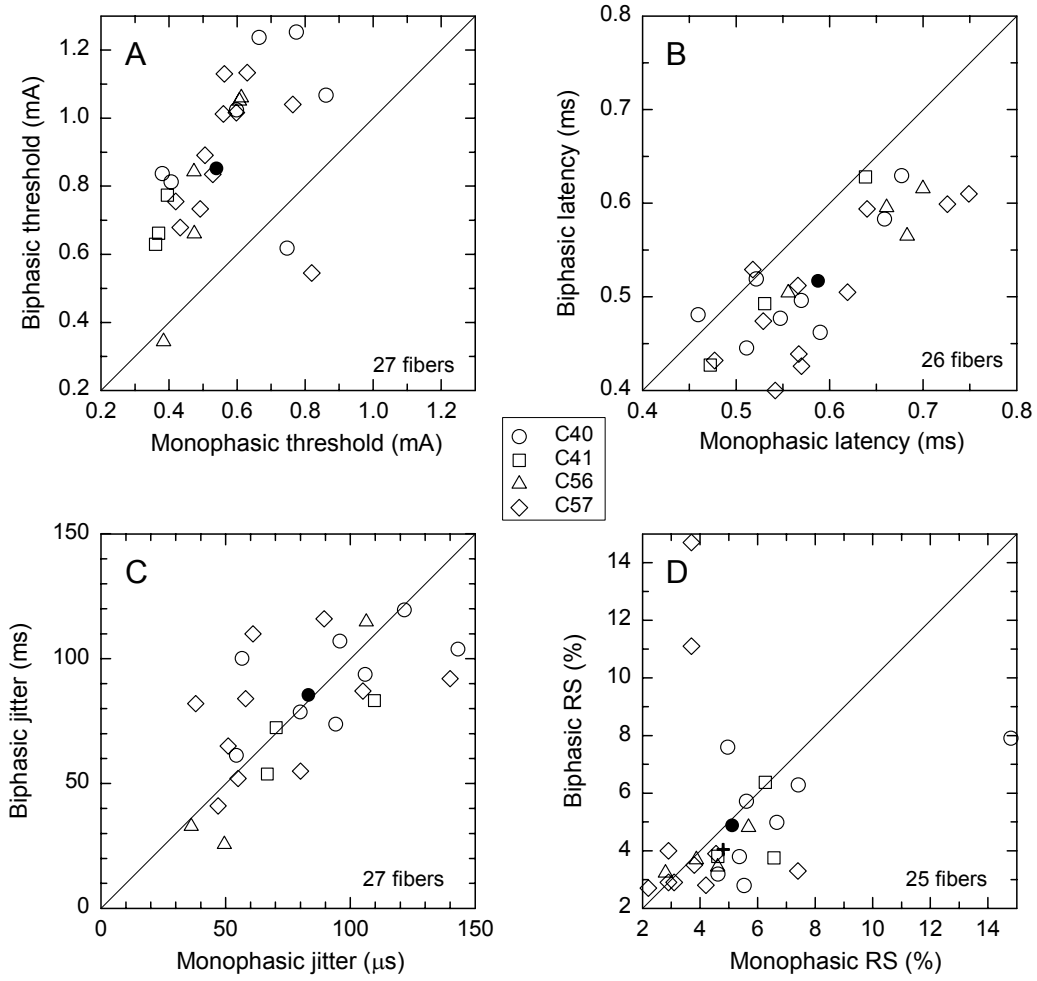

Figure 3 Summary of auditory-nerve single-fiber measures obtained using both biphasic and monophasic stimuli. Individual data from 16 fibers of 3 cats are shown by open symbols; mean values are shown by the solid symbols. Threshold, latency, and jitter were all defined for the condition of a firing efficiency of 50%.

single-fiber refractory properties was reported in Miller et al. (2001b), where (1) threshold, (2) jitter, (3) mean spike latency, (4) relative spread, and (5) spike amplitude were analyzed as a function of MPI.

Figure 4 shows how threshold and the other four properties varied with MPI. Data for individual fibers are plotted with solid dots, while mean values are plotted with open circles. For each of the five scatter plots, the data were normalized to the unmasked state and fit to smooth functions. In all but one plot (latency vs. MPI), statistically significant functional relationships were found. Our analyses of threshold recovery indicated the average fiber had faster recovery characteristics than had been reported previously. The mean recovery time constant was about 410 μs and the mean absolute refractory period was about 330 μs. Indeed, 13 of 34 fibers could respond when stimulated by a pulse pair separated by only 500 μs. Another intriguing finding was that RS increased at small MPI values. This phenomenon is relevant to cochlear implant stimulation, as most prostheses excite fibers with high-rate, repetitive stimuli, which presumably place fibers in states of partial refractoriness. Furthermore, we found significant decreases in spike amplitude during the refractory period (up to a 40% reduction), suggesting that the strength of neural activity may have reduced representation in the central nuclei. This dimension of neural encoding has not been widely considered as an important input variable to the ascending system. These data illustrate the importance of considering supra-threshold changes in several response properties when assessing the effects of prior stimulation.

Relationship to model results (QPR11)

Model simulations reported by Mino et al. (QPR11) assessed refractory properties in the model calculation algorithm described in Mino et al. (2002). That report described model responses to two-pulse stimuli and observed the effects of interpulse interval on threshold, latency, jitter and relative spread as shown in Figure 5. All parameters tended to increase with decreasing interpulse interval, suggesting that relative refractory properties can enhance the temporal variation in spikes. They also demonstrated that refractoriness can enhance the spatial spread of spike initiations. Responses were generally similar to effects observed in single fibers (Miller et al., 2001b). Such data suggest that even though refractoriness has been thought to limit the performance of neurons, refractory properties may be positively utilized to improve information transfer on neurons (Berry and Meister, 1998).

Alternative technique for stimulus artifact reduction with cochlear implants (QPR1)

Recording a compound action potential in response to electrical stimulation requires attention to minimize contamination due to electrical stimulus artifact. In patients implanted with the Nucleus 24 device, the ECAP is recorded using a neural response telemetry (NRT) system. This system employs a forward-masking technique that greatly reduces stimulus artifact (Brown & Abbas, 1990; Brown et al., 1990). Our data and that of others (Finley et al. 1997) examining ECAP responses to two-pulse stimulation have demonstrated variations in response waveform morphology as well as decreased amplitude. Such data demonstrated that the standard forward-masking technique in use in the Nucleus® NRT system can distort the ECAP waveform when the stimulated nerve is in a condition of partial refractoriness. In the cat, we demonstrated that this distortion affects the forward-masking recovery curves. Based on that data, a modified technique was introduced (Miller et al, 2000) that adequately reduces stimulus artifact but does not result in distorted recovery curves. It does so without appreciably increasing data collection time, an important clinical consideration. In some cases, the modified technique produced clearer ECAP waveforms than obtainable with the standard method. This technique has been implemented in a number of studies assessing both refractory properties as well as channel interaction using the Nucleus NRT system (Cohen et al, 2001; Abbas et al, 2003; Charasse et al., 2003; Xi et al., 2003)

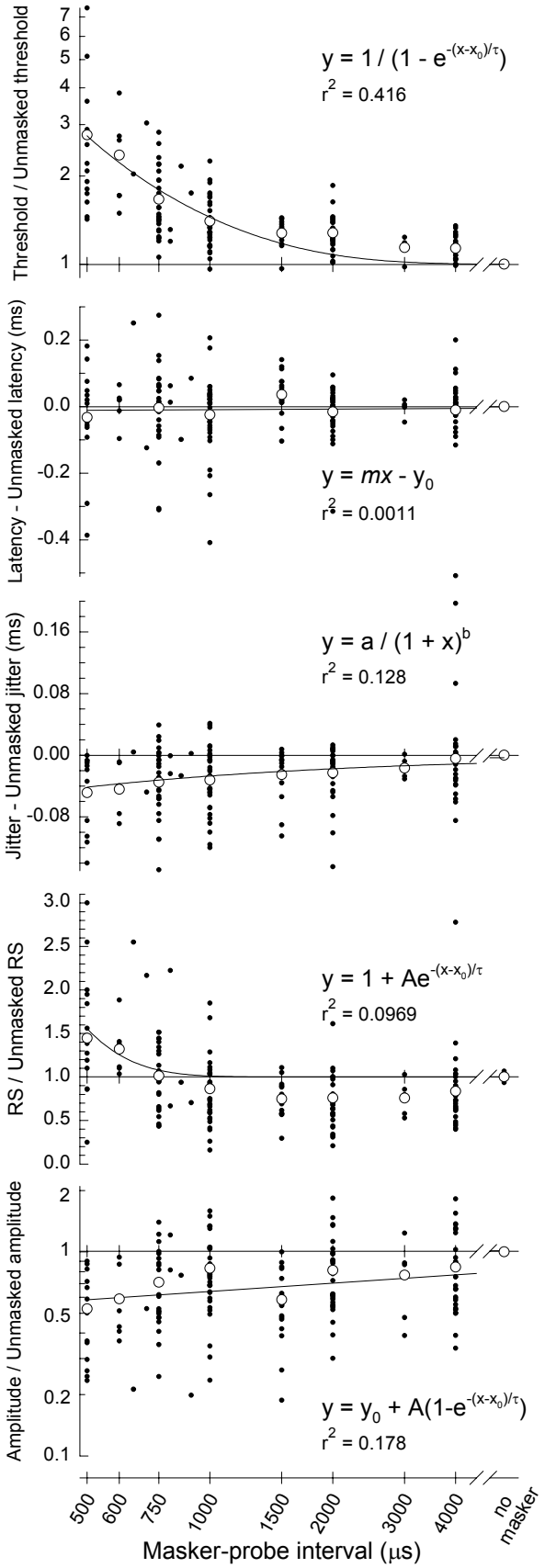

Figure 4 Summary data describing the refractory recovery properties of feline auditory nerve fibers. Five measures -- threshold, mean latency, jitter, RS, and amplitude -- are plotted for 34 fibers as a function of MPI. For each measure, the data for each fiber was normalized to the value obtained under the no-masking condition. Each scatter plot was fit to a function (the form of which is listed in each panel) in order to assess whether or not each dependent variable was significantly correlated with MPI. These fits are also plotted and the amount of variance explained (r^2) is listed in each panel. Mean values data at specific MPI values are indicated by open circles.

All measures (except RS) were assessed for the response condition of a firing efficiency of 50% (with data interpolation used when necessary)

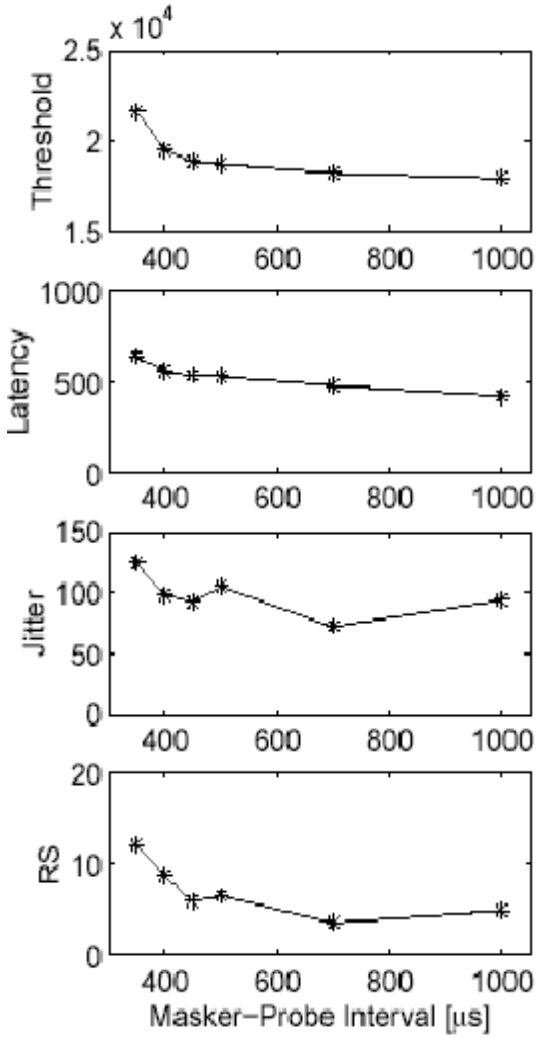

Figure 5 Results of a two-pulse refractory study using a biophysical computation model of a feline auditory nerve fiber. Parameters of simulated neural response are plotted as a function of masker-probe interval. Threshold (uA), latency (us), jitter (us), and relative spread (%) are plotted for electrode-to-fiber distance of 7 mm.

V. Responses to electric pulse train stimuli

ECAP responses to constant amplitude pulse trains (Contract N01-DC_6-2111)

To assess cumulative effects of repeated stimulation, we measured ECAP to trains of pulses that were typically over 100 ms in total duration. We systematically examined the effects of stimulus level, interpulse interval (IPI), and stimulus waveform on the pattern of pulse-train responses (Matsuoka et al., 2000a,b). Pseudomonophasic and biphasic pulse trains from both guinea pigs and cats evoked qualitatively similar response characteristics. The response typically showed refractory effects in that the response to the second pulse was smaller than that to the first pulse. In addition, the response to successive pulses showed an alternating pattern, as well as an overall decrease in response amplitude, likely the result of refractory recovery and cumulative adaptation effects, respectively. The amplitude alternation was highly dependent on IPI, with the greatest degree of alternation occurring at IPIs near 1 ms. While response patterns recorded from our cats and guinea pigs were qualitatively similar to those of implant patients (Wilson et al. 1995; Wilson et al., 1997), we consistently observed smaller-amplitude alternations in our animal preparations, as has Haenggeli et al.(1998). Also, in contrast to findings from humans, these alternations decayed faster, i.e. in animals, the pattern typically decays within approximately 50 ms where in human recordings the alternation typically persists for at least several hundred ms. We hypothesized that both of these differences are due to differences in the stochastic properties of the neurons excited in our animal preparations and in the human subjects. We speculated that higher noise levels exist in the neural membranes of acutely deafened animals and that this greater noise may result in more stochastic response patterns.

Long-term adaptation (QPR8)

Our previous work showed indications of long-term adaptation. For instance, single-fiber data demonstrated long-term changes in sensitivity after stimulation over the course of several minutes. Those changes were particularly evident with monophasic anodic stimulation and were related to stimulation rate (Miller et al., 1999a). Under this contract, we investigated those effects in more detail (Abkes et al., 2003). We observed the responses to continuous pulsatile stimulation to more carefully evaluate the time course of such changes. Because we record ECAPs with an electrode positioned on the nerve, we can (at some stimulus levels) record ECAP waveforms in response to individual pulses, without the need for time-averaging techniques. This approach allowed us to avoid measurement contamination from prior stimulation.

Figure 6 plots the ECAP amplitudes for each pulse of a long-duration (30 s) pulse train presented at an interpulse interval of 2 ms. A large decrement in the ECAP amplitudes is observed over a period of about 30 seconds. Smaller, though significant, decrements were also observed at slower pulse rates. The point-to-point amplitude variations are primarily due to the lack of signal averaging. The effect of pulse rate is shown in Figure 7. We plot the decrease over the 30 s period (asymptotic amplitude/initial amplitude) as a function of pulse rate for three different stimulus levels expressed as a percentage of the dynamic range. The data demonstrate a significant decrease in the responsiveness over time for IPIs as long as 20 ms.

Data such as these led us to investigate effects of presentation rate with pulse trains for cases when signal averaging is used. In those experiments, we fixed the pulse rate at 1000 pulse/s and the train duration at 100 ms. We then measured the averaged response with systematic changes in the inter-train interval. Data were collected from a guinea pig (M64) and a cat (D02) for several stimulus levels. Figure 8 plots the ECAP amplitude (normalized to the amplitude at the longest inter-train interval) as a function of inter-train interval. These data suggest that there can be a significant decrease in responsiveness for intervals as long as 400-500 ms.

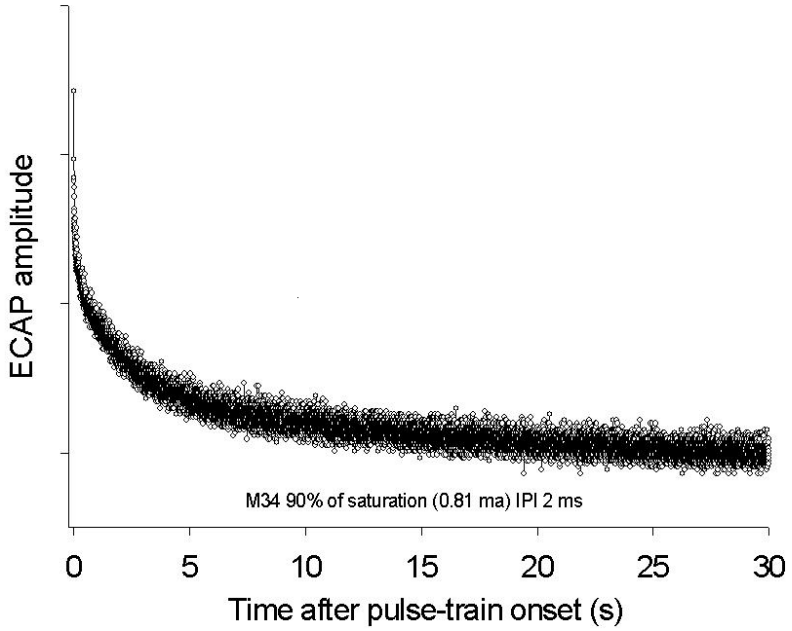

Figure 6 Results of a study using an acute guinea pig preparation on the effects of interpulse interval on ECAP responses to pulse-train stimulation. Responses were evoked using brief (40 us/phase) current pulses presented to a monopolar intracochlear electrode. Amplitude of the ECAP in response to each successive pulse in a train is plotted as a function of time relative to onset of the pulse train. The interpulse interval is 2 ms and the current level is 0.81 mA, which, in this subject elicited an ECAP of approximately 90% of the dynamic range.

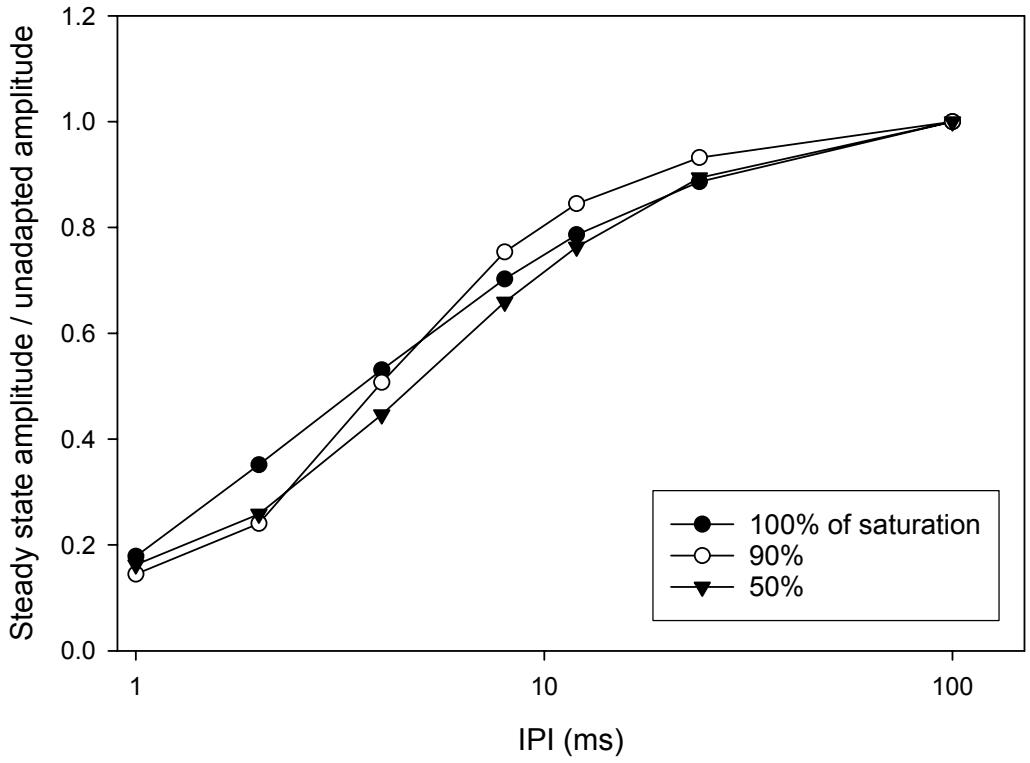

Figure 7 The effect of interpulse interval (IPI) on the degree of ECAP amplitude decrement across the duration of pulse-train stimulation. The decrease in ECAP amplitude over the duration of a pulse train is plotted as the asymptotic amplitude divided by the initial amplitude as a function of IPI. Data were obtained from an acutely deafened guinea pig subject and brief (40 us/phase) stimulus pulses were presented to a monopolar intracochlear electrode. Functions are plotted for 3 different levels: one evoking an ECAP of 50% of the dynamic range, the second evoking an ECAP amplitude of 90% and the third a maximum response amplitude.

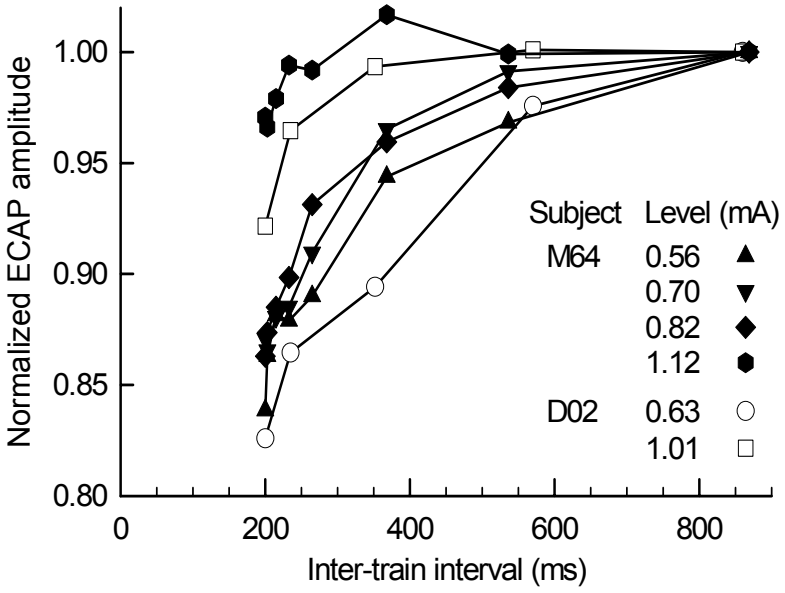

Figure 8 Effect of inter-train interval on the ECAP amplitude evoked by the first pulse a train of pulses. The ECAP amplitude to the first pulse has been normalized to the amplitude evoked using longest intertrain interval. Data are plotted for two different subjects (guinea pig M64 and cat D02) and at several stimulus levels as indicated in the legend. Duration of the pulse trains was 100 ms. Effects across successive pulse-train presentations are evident for "silent" intervals of at least 300 ms and longer in some cases.

Clinical considerations

The effects of long-term adaptation are relevant to mechanisms of electrical stimulation but also could be important for clinical use of ECAP measures in implant users. We note that both short-term and long-term effects are based on direct stimulation of the neural membrane and are not the results of synaptic effects. These results may also be relevant to clinical measures particularly considering that the neural systems of some users are likely impaired by chronic degenerative effects. Measurements using the Nucleus NRT system to record the ECAP have demonstrated similar short-term and long-term adaptation effects. Furthermore, we have observed significant variations in the decrease in ECAP amplitude over time across different subjects as well as across stimulation electrodes within a subject. We typically noted changes in amplitude at rates as low as 80 pulse/s, a rate which is typical for recording of the ECAP with NRT, suggesting that adaptation may affect response amplitude for many recording situations. Also, since there are significant variations in adaptation, we expect that the degree of adaptation may be an indication of the condition of stimulated neurons and may also be indicative of the input to the CNS relative to psychophysical tasks such as temporal integration.

An important issue relative to the use of ECAP measures in clinical populations has been the prediction of behavioral thresholds from physiological measures. The rationale for examining such measures is the application to young children or impaired individuals where behavioral measures of threshold and uncomfortable loudness may not always be possible. Since the behavioral measures of interest are in response to relatively high rate pulse trains, temporal integration is an important determinant for behavioral threshold. For ECAP measures the response is measured to single pulses so that temporal integration is not a factor. As a result, the difference between ECAP threshold and behavioral threshold is at least partly determined by temporal integration (Brown et al., 1999). If measures of adaptation can provide a more accurate evaluation of the input to the temporal integration mechanism, then they may be helpful in providing a better estimate of behavioral threshold using ECAP measures.

High-rate conditioning stimuli (QPR4, QPR10)

In research under our previous contract (Rubinstein et al., 1999), we reported simulations of single-unit recordings to stimuli consisting of a 1-kHz sinusoid in association with a 5-kHz monophasic pulse train. The pulse train was referred to as the "conditioning" stimulus, as it was conditioning the nerve fiber to produce pseudospontaneous activity. Without the conditioning stimulus, the fiber responded in a highly synchronous manner, primarily to the peak of the sinusoid. The presence of the conditioning stimulus was found to improve the dynamic range of rate-level functions, and to improve the temporal resolution of the fiber's response to the sinusoid by allowing the fiber to respond to most of the waveform changes over time. The addition of the conditioning stimulus resulted in simulated responses that resemble neural responses to acoustic stimuli. Based on those model results, Litvak (Litvak et al., 2001; Litvak, 2002) performed experiments demonstrating similar effects in single auditory nerve fibers.

As a part of this contract work, we conducted a series of experiments to evaluate the effect of a high-rate (“HR”) conditioner on the response to continuous analog (sinusoidal) stimulation (Runge-Samuelson et al., 2001a,b). The ECAP in response to 100 Hz sinusoidal stimulation was recorded both with (“sine+HR” condition) and without (“sine-alone” condition) the simultaneous presentation of high-rate pulse train (5000 pulse/s train of 40 μs/phase biphasic pulses). We found that the morphology of the ECAP in response to a sinusoid varied with stimulus level so that simple measurements of peak amplitude and latency may not appropriately characterize the response. The magnitude of the ECAP was therefore calculated as the RMS value across the response period. In Figure 9 (panel A), the growth of response amplitude with sinusoidal level is shown for the sine-alone and the sine+HR conditions. The boxed areas highlight the response

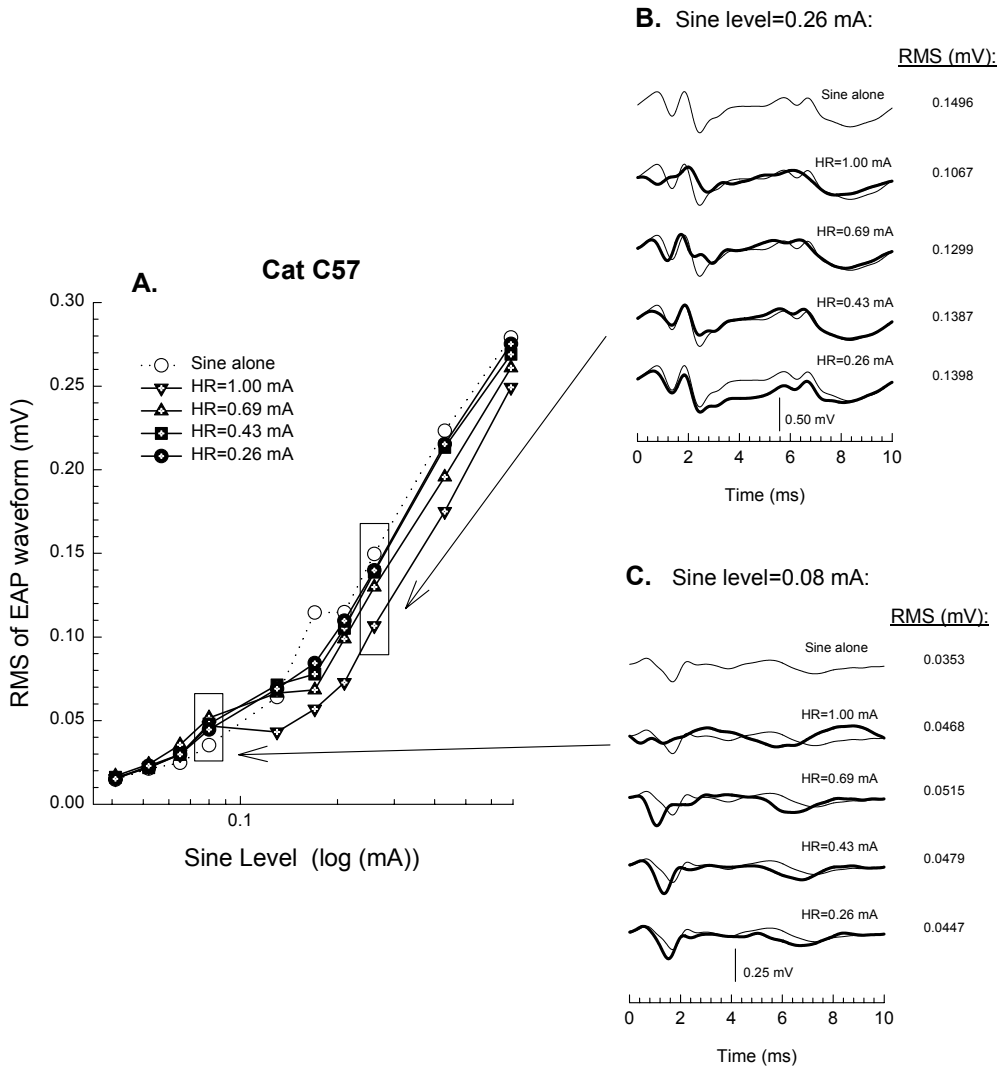

Figure 9 Results of a study of the effects of a high-rate electric pulse-train stimulus on the auditory nerve response to sinusoidal electric stimuli. Data are from an acutely deafened cat. Panel A: Response amplitudes, derived from the RMS value of the response waveforms, are plotted as a function of the sinusoidal level for cat C57. The boxed areas emphasize the response amplitudes for a moderate (0.26 mA) and a low (0.08 mA) sinusoidal stimulus level.

Panels B and C: Recorded response waveforms corresponding to the two levels highlighted in panel A. Thin lines correspond to sine-alone condition, thick lines to sine+HR condition. In each case, the parameter is the level of the high-rate pulse train. The response amplitudes to the sine-alone and the sine+HR are shown next to the corresponding waveforms.

amplitudes in response to a moderate level (0.26 mA) and a low level (0.08 mA) of sinusoid. Those levels were chosen to demonstrate the general trend that, in the presence of high-rate stimulation, response amplitudes to the sinusoid are larger at low levels and are smaller at moderate and high levels. Response waveforms for those stimulus levels illustrated in Figure 9 (panels B and C) demonstrate these trends. These data are generally in agreement with a hypothesis that addition of the high-rate pulse train increases sensitivity to the sinusoidal stimulus and decreases the slope of the growth function, consistent with an increase in dynamic range.

Modeling work and results such as those described above have led to perceptual measures in human implant users investigating the perceptual dynamic range in response to similar stimuli with a background conditioner. Those results have demonstrated a significant threshold decrease with conditioner resulting in an average of a 7 dB increase in dynamic range with presentation of the conditioner (Hong et al., 2003). More recently, effects of conditioning stimulus on frequency discrimination have been assessed (Meyer et al., 2003). In addition to such applications with speech processing for cochlear implants, Rubinstein et al. (2003) are also evaluating the use of high-rate electrical pulsatile stimulation as a means of tinnitus suppression.

Responses to amplitude modulated stimuli

In contrast to constant-amplitude pulse trains, amplitude-modulated trains provide a more realistic simulation of CIS-like stimulation. We have used our animal models to measure the ECAP to such stimuli and assess the degree to which the modulation in ECAP amplitude follows the modulations in the stimulus (Abbas et al., 1998). At relatively low modulation depths, an approximately sinusoidal modulation of response amplitude was observed. At higher modulation depths, the response pattern had correspondingly larger variations, but the pattern became distorted from that of a sinusoid. Such distortions suggest a degradation in the ability of nerve fibers to encode stimulus modulations. The degree to which the central system is unable to "decode" these distortions represents a challenge and opportunity for improved stimulus encoding. Additional research would be needed to determine the extent to which such peripheral distortions present an obstacle to perception.

In the previous contract, we reported on preliminary data using amplitude-modulated pulse trains to evoke the ECAP at frequencies from 50-400 Hz. Those data showed a clear modulation in the response amplitudes for modulation depths as low as 1%. During the present contract period, we systematically assessed the effects of modulation frequency. To measure the effects of modulation frequency over a larger range it is necessary to use a relatively high rate carrier frequency. However, at rates above 1000 pulse/s, the neural response to each pulse in the train is not clearly distinguishable, necessitating a time-consuming subtraction procedure (Wilson et al., 1997). We used a carrier rate of 5000 pulse/s to assess modulation frequencies up to 1600 Hz. Examples of modulation of the response as a function of modulation frequency for a fixed carrier level are shown in Figure 10. The response tends to be larger for modulation frequencies 200 Hz and above. Psychophysical data reported with cochlear implant users typically show a decrease in modulation detection for frequencies above 50-100 Hz (Busby et al, 1993; Shannon, 1992). Such data suggest that the peripheral response to temporal modulation is robust even at frequencies where modulation perception is diminished. The extent to which the high-frequency peripheral responses may affect the perception of complex signals, such as music, is not clear however.

Finally, under the no-cost extension period of this contract, we began investigating the possibility of using the steady-state evoked response to electrical stimulation to assess a more central response to modulation that may be applicable in human implant listeners. The steady state evoked potential in response to acoustic stimulation has been reported on extensively in both human and experimental animals (Galambos et al., 1981; Kuwada et al., 1986; Dolphin and Mountain, 1992). The response can be separated by the artifact as the stimulus waveform does not contain energy at the modulation frequency and the response is

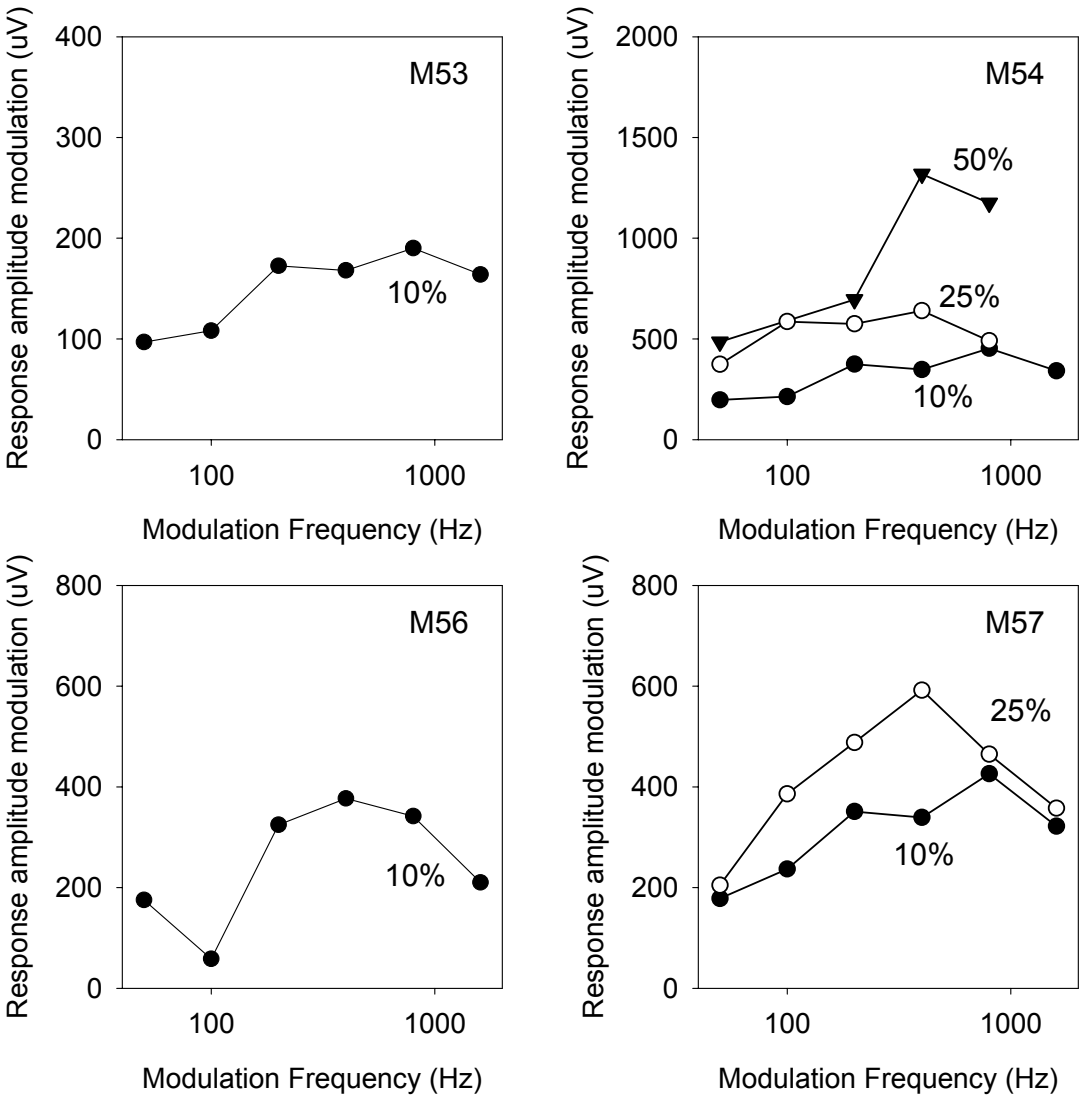

Figure 10 The effect of modulation frequency on the degree of modulation evident in the ECAP response. Data were obtained from 4 guinea pig subjects. The modulation in the response amplitude of the ECAP is plotted as a function of modulation frequency. A modulation depth of 10% was examined in all four subjects; additional depths were examined in two subjects, as indicated in each graph. Modulated electric pulses were presented at a rate of 5000 pulse/s.

dominated by the modulation frequency and its harmonics. It is therefore a relatively straightforward way of recording responses to modulated stimuli. We have recently reported use of a similar methodology to record an electrically evoked potential in guinea pigs (Jeng et al 2003). The application to humans could be particularly important in that such a response could provide a more central assessment of responsiveness to modulation.

VI. Spread of excitation / channel interaction

In the final report from the previous contract (Contract N01-DC-6-211), we described recordings of compound action potentials in cat where we used a two-pulse forward masking paradigm to assess channel interaction. That paradigm assessed the effect of a masker pulse on the response to a probe as masker electrode was varied across a multi-electrode array. Based on further analysis of that data, Miller et al (2001a) suggested a refinement of the method for assessing channel interaction using the ECAP. We noted that by choosing level of the masker to elicit a constant response across electrodes, a more parsimonious interpretation of the interaction among stimulating electrodes resulted.

Clinical application

That paradigm has since been applied in studies assessing the channel interaction effects in cochlear implant users (Abbas et al., 2002, 2003; Xi et al., 2003). The results of those studies have demonstrated a range of spatial selectivity functions across individuals, as well as across implant types, i.e., Nucleus Contour vs. Nucleus banded array. In addition, we have demonstrated differences in spatial selectivity with different intracochlear electrode configurations (Abbas et al., 2003).

In our clinical studies conducted in parallel with this contract work, we have found that, in many implanted individuals, monopolar stimulation can result in channel interaction patterns limited to a relatively narrow region of the electrode array such that there can be electrode combinations with no measurable interaction between two monopolar sites. This somewhat surprising result contrasts sharply with a widely accepted view that monopolar stimulation provides little or no spatially selective nerve activation (cf. van den Honert and Stypulkowski, 1987). It should be noted, however, that some single-fiber studies have demonstrated spatial selectivity with monopolar intracochlear stimulation (Miller et al., 1997; Liang et al., 1999). The discrepancies among these reports could be attributable to both the spatial dimensions of the stimulating electrode and its position within the three dimensional space of the scala tympani (Shepherd et al., 1993).

VII. Effects of stimulus electrode configuration on neural excitation

Some implant users have been reported to achieve better speech perception with monopolar or “wide bipolar” configurations (Pfingst et al., 1997; Pfingst et al., 2001). One explanation for better monopolar performance, forwarded by White and others (White, 1984; Smith & White, 1995; Pfingst et al., 1997), appeals to a spike-count model for the neural encoding of loudness. With this model, a particular loudness percept is encoded as a fixed number of spikes from the auditory nerve, although that spike count could be transmitted by various configurations of fiber populations. To maintain the same percept with monopolar and bipolar stimulation, the monopolar mode would activate a greater number of fibers, but each at a lower firing efficiency. In this context, electrode configuration influences spatial spread of neural activity and, by

doing so, influences stochastic response properties such as firing efficiency and jitter (cf. Miller et al., 1999a, Figure 4).

Based on these issues, we conducted a study using the ECAP to assess monopolar/bipolar comparison using a Nucleus-type banded electrode array (Miller et al., 2003). Example ECAP waveforms are shown in Figure 11. All waveforms are "raw" responses (i.e., not processed by any artifact reduction scheme) and were evoked using cathodic stimuli presented to electrode 1 (the most apical). Stimulus levels are indicated in each case. Typical ECAP waveforms elicited by monopolar stimulation were characterized by a dominant negative potential (N1) and subsequent positive peak (P2) occurring within the first 1 ms after stimulus onset. In some cases, an earlier P1 peak can be seen. When comparing the upper two sets of waveforms, note that monopolar responses (left panel) occurred at lower stimulus levels and grew more precipitously. More complex ECAP morphologies were observed in three of our subjects with bipolar stimulation; examples from two cats are shown in the lower panels. As stimulus level was increased, ECAP morphology changed in a discontinuous manner, with the appearance and growth of an earlier negative component. We believe that these bipolar ECAPs reflect the shifting of excitation from the peripheral process at low levels to the central process at higher levels. This pattern resembles the bimodal ECAPs and appearance of an "N0" peak reported by Stypulkowski & van den Honert (1984), although that study did not examine stimulus electrode configuration effects.

In most cases, the ECAP amplitude-vs.-level functions for monopolar stimulation can be characterized by sigmoidal functions. To facilitate across-animal comparisons of monopolar and bipolar growth functions, the functions were normalized so that the monopolar functions intersect each other at the 50% point and so that they saturate at a value of 1.0. The bipolar growth functions were normalized by the same factors used for the monopolar functions. The normalized functions are shown in Figure 12, with thick lines representing the mean values of the monopolar and bipolar growth functions computed across six cats. These functions demonstrate the greater dynamic range produced by bipolar stimulation as well as the prominent low-level tails with bipolar stimulation that are not evident with monopolar stimulation.

While these differences in monopolar and bipolar growth have been known for decades (primarily through EABR measures), our ECAP data provides new information regarding the underlying mechanism. First, we noted that the transition from the late ECAP latency to the early ECAP response typically occurred at the "knee" of the bipolar functions. We speculate that the two regions of bipolar growth correspond to the two excitation sites. Comparisons of ECAP latency are made through plots of latency versus ECAP amplitude. If we assume that ECAP amplitude reflects the number of responding fibers (e.g., Miller et al., 1999b), such plots provide a means of assessing latency as a function of the population response. Such plots are shown for all subjects and both polarities in Figure 13. N1 latency is plotted versus normalized ECAP amplitude, in which both monopolar and bipolar ECAP amplitudes were normalized by the maximum (i.e., saturation) amplitude achieved with monopolar stimulation for each subject. While there is variability across animals, some trends are evident. Three subjects (C88, C90 and C98) produced bipolar latency functions marked by precipitous drops in N1 latency while a fourth subject (C75) demonstrated a similar effect with tripolar stimulation. Notably, with low stimulus levels, each of these four cases of relatively focused stimulation produced the largest observed N1 latencies. While more prevalent with cathodic stimuli, sharp N1 shifts were observed in two subjects with anodic stimulation. Note that the responses of subjects C75, C88, C90 and C98 undergo large latency drops at response amplitudes between 1 and 10% of maximum amplitude. These particular plots are emphasized by the filled symbols.

These bipolar ECAP growth and latency functions suggest that localized recruitment and excitation of the peripheral processes produced response amplitudes as large as 10% of that measured at monopolar saturation. Thus, these data are consistent with a hypothesis that a large subpopulation of fibers can be excited at their peripheral processes with focused bipolar stimulation.

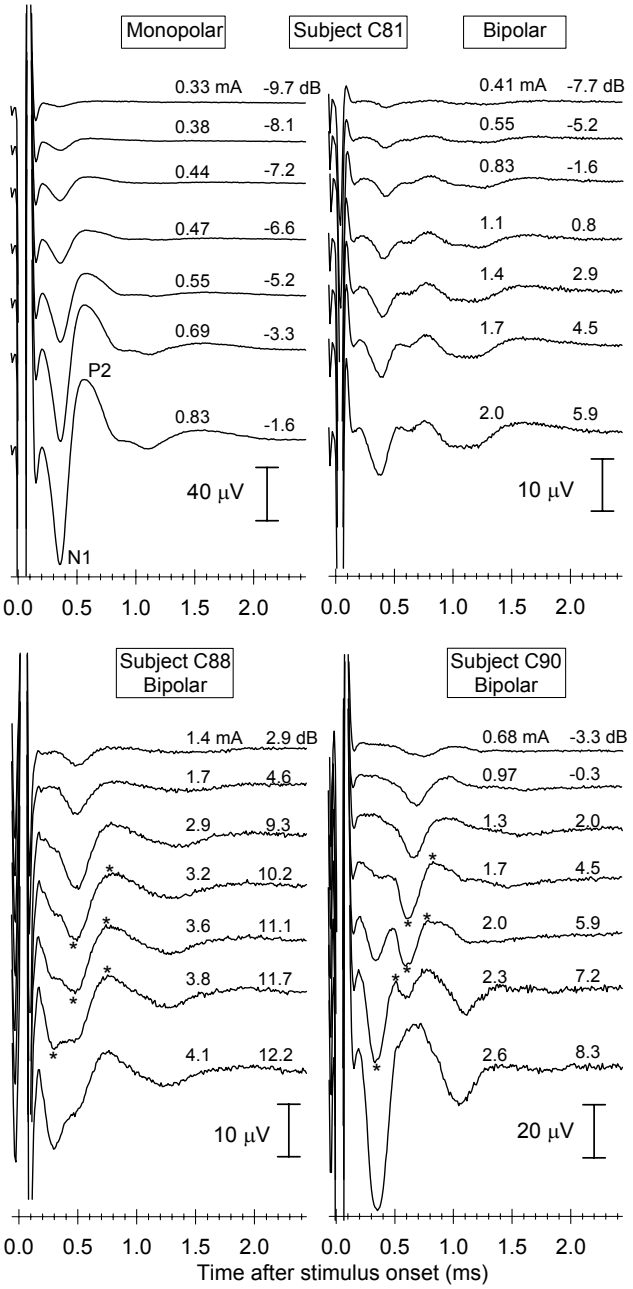

Figure 11 Examples of ECAP waveforms from three cats. For each waveform, stimulus levels are shown in both linear and dB units (relative to 1 mA). Each waveform demonstrates a large stimulus artifact that occurs within the first 0.1-0.2 ms. The prominent negative component (N1) and subsequent positive component (P2) are labeled in one waveform of the upper left panel. Some traces also show evidence of later potentials (occurring after 0.8 ms) that are attributed to the cochlear nucleus. **Upper panels**: ECAPs from one subject produced by monopolar (left) and bipolar (right) stimulation. **Lower panels**: ECAPs from two subjects produced by bipolar stimulation, demonstrating a discrete, level-dependent change in ECAP morphology and latency.

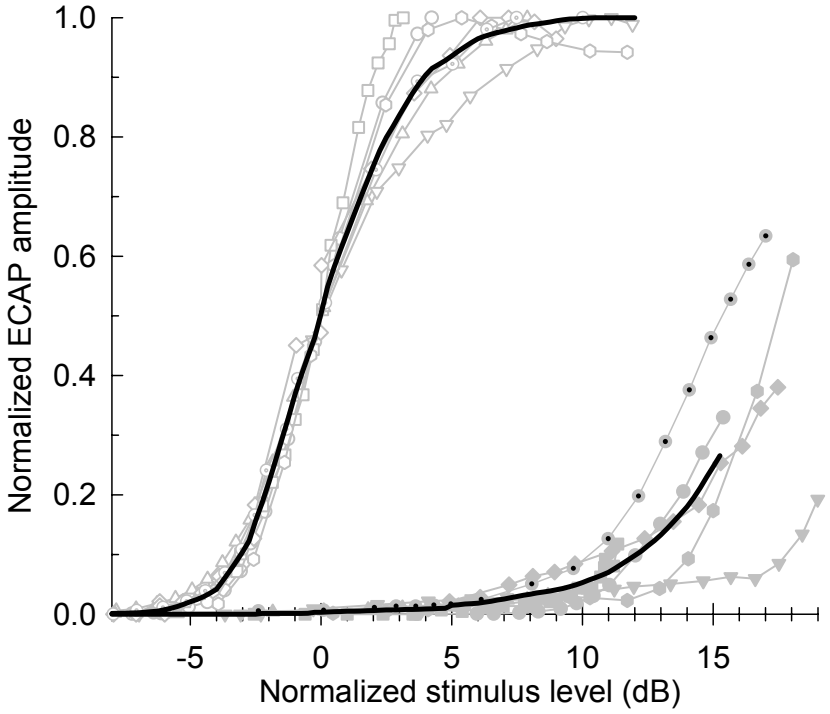

Figure 12 Normalized ECAP growth functions for monopolar (open symbols) and bipolar (filled symbols) electrode configurations. Data are shown for a total of seven cats. Thick solid lines indicate the mean values computed over data from five subjects stimulated with monophasic pulses up to a level of 15 dB. All functions have been normalized to the monopolar growth functions (as described in the text) to facilitate across-subject comparisons.

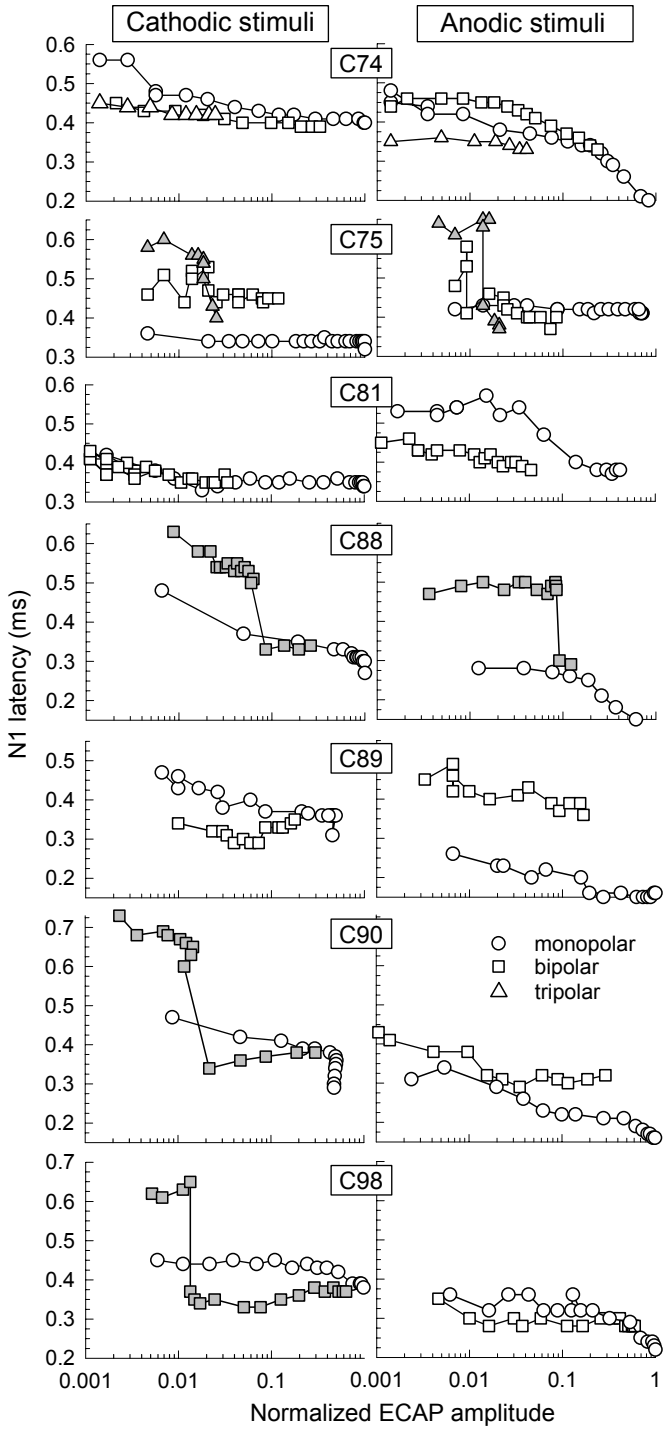

Figure 13 Plots of ECAP N1 latency as a function of normalized ECAP amplitude. For each of the seven cat subjects, ECAP amplitudes were normalized to the maximum amplitude obtained from that subject with monopolar stimulation. Grey symbols highlight functions that exhibit discrete shifts in N1 latency, corresponding to double-peaked ECAP waveforms.

Clinical relevance

A means of assessing the site of action potential initiation could have clinical value for two reasons. First, greater knowledge of site-of-excitation could provide motivation for improved stimulus control to "steer" excitation to specific neural sites. Such control could reduce so-called "ectopic" excitation of fibers or avoid anomalous excitation in specific cases. Our data suggest that the ECAP could provide the relevant electrophysiologic assessment tool. Second, chronic degenerative effects secondary to deafness leads to a slow progression of neural loss that includes loss of peripheral processes and myelination. A means of determining how such progressive effects influence site-of-excitation may be valuable. Peripheral electrophysiologic measures could, therefore, provide a more detailed assessment of neural status across time.

VIII. Effects of recording electrode position on the ECAP (QPR12)

The majority of animal research of the electrically evoked compound action potential (ECAP) has been based upon recordings obtained from electrodes positioned on or near the surgically exposed nerve trunk or some other extracochlear site (Stypulkowski & van den Honert, 1984; Killian et al., 1994; Miller et al., 1998; Haenggeli et al., 1998). While there are strong technical and theoretical reasons for doing so, such recording sites differ from the intracochlear sites employed when recording from cochlear-implant users equipped with clinical "NRT" or "NRI" systems. We therefore conducted a study, reported in QPR11 where details of the methods and results are presented. In those experiments we measured the responses at different cochlear locations using a multi-electrode array. We also compared those results to data recorded from different locations near the auditory nerve.

The largest differences were observed among intracochlear electrodes using bipolar stimulation. In those cases we used the two most apical electrodes in a banded electrode array for stimulation and other electrodes for recording. We noted discrete shifts in amplitude and latency functions attributable to differences in the ECAP initiation site. As noted earlier, the corresponding latency data suggest a peripheral site of initiation corresponded to a relatively large intracochlear potential, consistent with the supposition that the peripheral processes pass close to the intracochlear recording sites. We also observed significant across-subject variations in the patterns of intracochlear ECAP recorded from our acutely deafened cat subjects. However, we have also observed a consistent trend of relatively large ECAP amplitudes recorded by intracochlear electrode I3, closest to the bipolar stimulating electrodes, at low stimulus levels. This is shown for three animals in Figure 14, which plots the normalized ECAP growth functions. Normalization of these functions was performed by dividing the intracochlear ECAP amplitudes by the corresponding ECAP amplitudes obtained using a nerve-trunk electrode, with the assumption being that the nerve-trunk electrode will record field potentials less biased by the effects of tissue partitioning such as what has been demonstrated with intracochlear recordings. We speculate that this greater representation of neural activity by electrode I3 is due to its relative proximity to the subset of fibers excited by the bipolar stimulating pair at those low levels. As fiber recruitment increases at higher levels, this electrode advantage disappears.

The examination of intracochlear electrode recordings in Figure 14 was based upon comparisons relative to ECAPs recorded using an electrode positioned directly on the surgically exposed nerve trunk. Although recording electrodes positioned on the nerve trunk may provide a less spatially biased representation of neural activation than would intracochlear recording electrodes, we must also assume that such nerve-trunk positions will also produce a distance-weighted representation of the excited neural population. By recording from different distances from the nerve trunk, we observed that the degree of

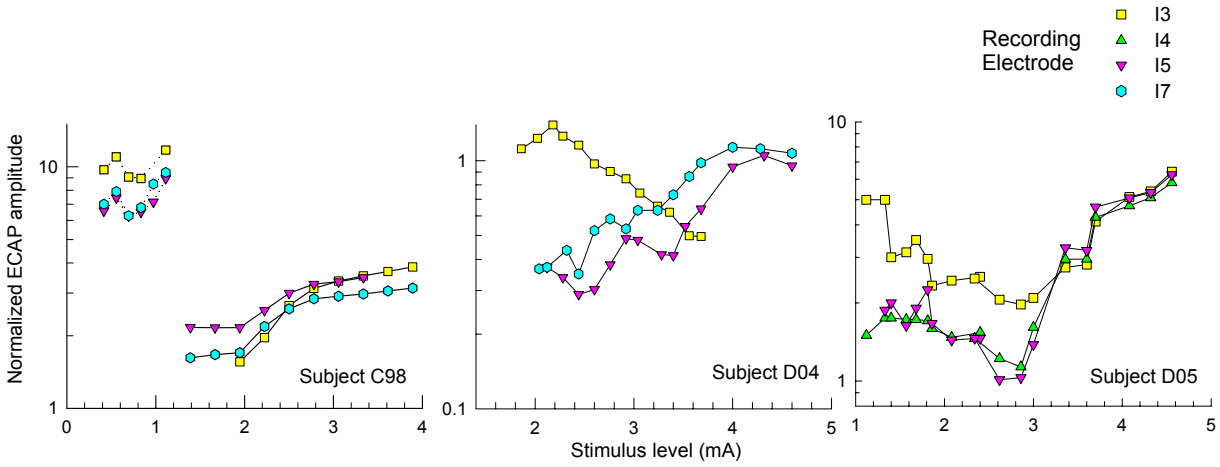

Figure 14 Normalized ECAP growth functions from 3 subjects for different intra-cochlear recording electrodes. A Nucleus-type electrode array with 8 banded electrodes was inserted into the scala tympani, with electrode I1 the most apical and electrode I8 the most basal. Bipolar stimulation was accomplished using I1 and I2. Other electrodes were used for recording as indicated in the legend. Amplitudes have been normalized to those obtained from the nerve-trunk electrode.

distortion increases as electrode-to-nerve distance decreases. In addition, the low-level responses have the greatest weight, since the bipolar stimulation likely excites a basal locus of fibers that are located toward the edge of the nerve trunk's cross section.

Clinical relevance

These results are relevant to research with animal models, but also suggest that the choice of the intracochlear electrode used to record human ECAPs (with "NRT" and "NRI" systems) may affect results. Specifically, by choosing a recording electrode close to the stimulating electrode(s), one might obtain ECAPs weighted toward a local subpopulation. In contrast, use of a more distant electrode may be more appropriate for more "global" ECAP measures. One interesting possibility is using intracochlear measures (perhaps along with an extracochlear site as a reference) in order to assess longitudinal changes in excitation patterns in a chronically implanted subject. These data suggest that the choice of recording electrode will influence any such assessment.

IX. Feasibility of thin-film recordings from the auditory nerve

Rationale

A series of experiments were performed to assess the feasibility of using silicon-substrate thin-film electrodes to record from multiple sites within the auditory nerve trunk. Recent studies have shown that multiple-electrode thin-film probes can provide spatial excitation maps of comparable quality to those provided by tungsten-electrode recordings at the level of the cortex (Arenberg et al., 2000) and the inferior colliculus (Arenberg-Bierer et al., 2002). This approach has also been successfully applied to cochlear-implant research. Specifically, multiple-electrode probes have made it possible to rapidly evaluate the spatial excitation patterns produced by various intracochlear stimulus electrode configurations (Snyder et al., 2003), thereby assisting in the evaluation of experimental configurations for potential use in future designs of cochlear prostheses.

The work described here was conducted to determine the feasibility of using thin-film electrodes in the trunk of the auditory nerve to provide information on the spatial extent of neural excitation at the peripheral level of the auditory system (a report on preliminary work appeared in QPR6). There are unique research benefits associated with recording evoked potentials from the auditory nerve. The transduction of cochlear-implant stimuli (depolarizing currents) occurs at the level of auditory nerve fiber membranes; therefore, the spatial and temporal response properties of the auditory nerve define the limits of information transfer from the prosthesis to the auditory system. As temporal response patterns within the auditory system tend to be more limited in spectral content at successive ascending neural stages (in part due to stimulus feature extraction), there is particular value in quantifying the degree of temporal information that is successfully encoded at the input of the auditory system. Responses from the nerve provide details, not observed at more central sites, that can provide insight on how electrical stimulation excites the auditory system. For example, as we noted earlier, the nerve's electrically evoked compound action potential exhibits unique temporal responses for different modes of intracochlear electrical stimulus delivery plausibly linked to different sites of action potential initiation (Miller et al., 2003). Such a means of assessing site-of-excitation could be useful to better control the delivery of electric stimulation and as a clinical tool for assessing nerve status.

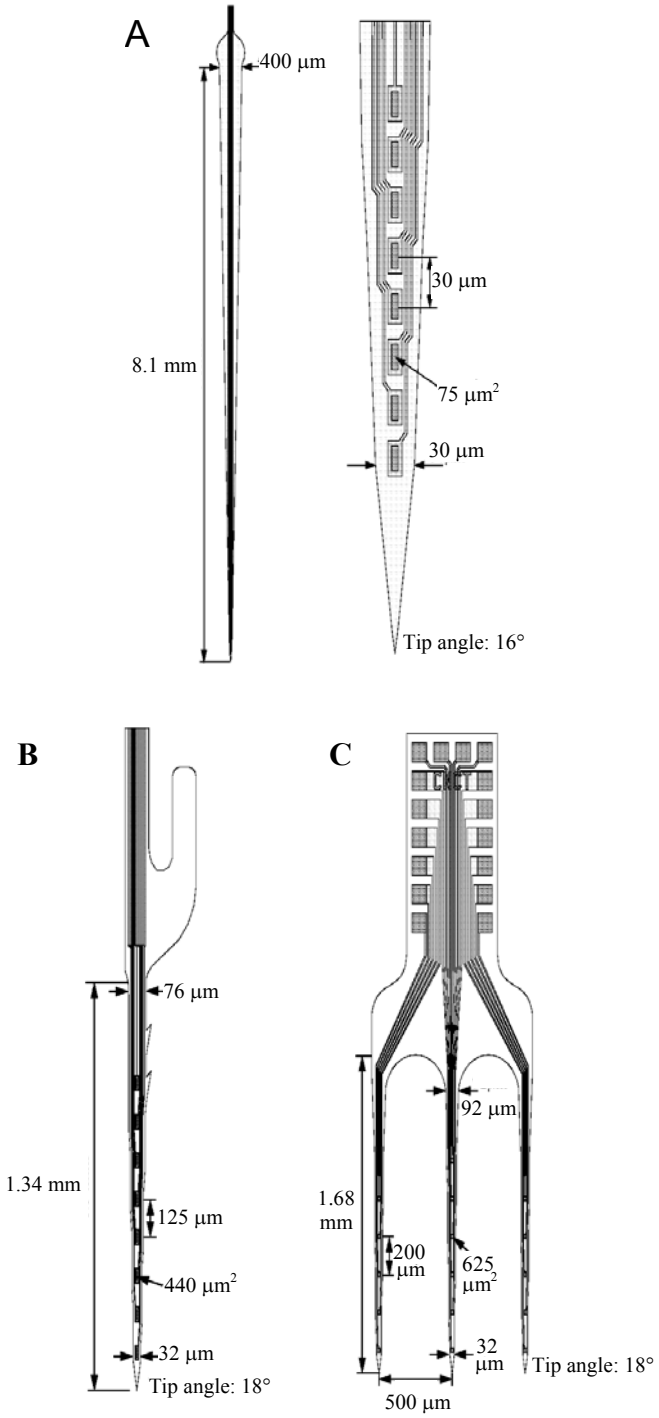

Figure 15 Mechanical drawings of the three configurations of thin film electrodes fabrication by the University of Michigan Center for Neural Communication Technology and used in our feasibility study. Two views of the NASA1 single-shank electrode are shown in A, the PSU4 probe is shown in B, and the three-shank array designed specifically for this feline study is shown in C.

The use of thin-film depth electrodes in the auditory nerve presents challenges, however. In contrast to recording from the inferior colliculus or primary auditory cortex, the fibers within the auditory nerve are not tonotopically ordered along a single axis or in a monotonic fashion. Auditory nerve fibers follow spiral paths within the trunk, resulting in relatively complex arrangements of best-frequencies that vary along the axis of the nerve (Sando, 1965). Furthermore, depth recording electrodes will contact relatively small diameter (2-5 mm) axons. The relatively large thin-film electrode surface areas (typically in the hundreds of square microns) may therefore make it impossible to establish intimate electrical contact with a small number of axons having similar characteristic frequencies.

The primary goal of this work was to determine the frequency selectivity of thin-film electrode arrays positioned within the auditory nerve with the cochlea excited by pure-tone stimuli. Ideally, each electrode site would be sensitive to a spatially limited subset of fibers, thereby producing unique frequency tuning curves that approach the degree of tuning observed for single fibers. We also examined the feasibility of inserting available thin-film electrodes into the feline nerve trunk and determining the extent of tissue damage due to insertion trauma. Using the more promising electrode designs (including two designed specifically for the feline nerve), we assessed the quality of the recorded potentials evoked by acoustic tone-burst stimuli. Finally, we also made recordings of electrically evoked responses. The results indicate that, although these electrodes do cause trauma from their insertion, thin-film electrodes with relatively small shank dimensions can be used to record auditory nerve potentials from within the nerve trunk. Assessments using tonal stimuli suggest that the place-specificity of the tested electrodes is too broad for assessment of the place of cochlear excitation, at least by relatively simple means of analyses. However, the electrodes do provide sufficient place-specificity for their application for estimates of neural conduction velocity.

Stimulation and recording

Tone-burst waveforms had a total duration of 5 ms, with linear onset and offset ramps of 1 ms each. A Beyer DT-48 earphone was coupled to a speculum fitted with a probe tube microphone that provided for the monitoring of canal sound pressure during the experiment.

The CNCT thin-film recording probes were connected to a multichannel unity-gain headstage by means of a standard dual inline package IC socket. The headstage/microelectrode probe assembly was, in turn, mounted into a Narishige micromanipulator. To maintain visibility of the auditory nerve, a small-profile headstage was custom-built using surface-mount components on a double-sided board. (Note: interested investigators may contact the authors of this report for information on this board design). The headstage amplifier design was based upon that provided by the University of Michigan CNCT group. The headstage outputs were amplified (1000x), low-pass filtered (15 kHz cutoff, 4-pole Bessel filters) and averaged.

The silicon probes were provided by the CNCT group, whose work was sponsored by NIH NIBIB grant P41-RR09754. Four different thin-film electrode designs were evaluated: (1) the NASA1 probe, a single-shank, eight-electrode array, (2) the PSU4 probe, a single-shank, eight-electrode array, and (3) a custom-fabricated three-shank, 16-electrode array and (4) a modified version of the three-shank array with smaller electrode pad areas. Physical dimensions these probes are shown in Figure 15. The two existing probe designs (NASA1 and PSU4) were chosen for their different inter-electrode pad spacing and electrode pad areas. The two three-shank electrodes were designed specifically for this study in an attempt to sample multiple neural sites within a two-dimensional cross-section of the feline auditory nerve trunk. The two versions of this probe design differed only in their electrode pad sizes.

Histological assessment

After completion of electrophysiological data collection, the auditory nerve trunk of two subjects (C86, C91) was dissected and preserved for histological assessment of trauma from probe insertion. C86 was perfused intracardially with fixative (2.5% paraformaldehyde / 1.5% glutaraldehyde buffered to pH 7.4 with 0.1M phosphate) after which the intracranial portion of the auditory nerve, including a portion of the cochlear nucleus, was dissected and immersed overnight in fresh fixative. At the end of data collection for C91, the nerve was removed and placed directly into fixative overnight without intracardiac perfusion. Following 8 – 12 hours of fixation, the specimens were rinsed in phosphate buffer and post-fixed in 1% phosphate-buffered osmium tetroxide with 1.5% potassium ferricyanide, dehydrated, and embedded in epoxy resin. Each nerve was then serially sectioned at a thickness of 1.5 micron, beginning at the end dissected from the internal auditory meatus, and proceeding to the cochlear nucleus. Sections were mounted on glass slides, stained with Azure B and methylene blue, coverslipped, and examined with a Nikon Labophot light microscope. The cross-sections of specimen C91 exhibited more fixation shrinkage than did those of C86; this was likely due to the lack of systemic perfusion.

Our initial goal was to determine electrode dimensions and properties suitable for insertion and use for acute (non-survival) feline experiments. Early attempts demonstrated that electrode shanks with widths greater than 40 μm could not be inserted into an orthogonal plane without large compressive deformation of the nerve. Furthermore, a probe tip angle no greater than 20 degrees provided easier insertion into the tissue. We therefore selected two single-shank CNCT probes with appropriate insertion footprints: the NASA1 and the PSU4 probes. In the first case (subject C86), a PSU4 single-shank probe was inserted only once in a plane orthogonal to the nerve axis. In this case, the probe array was positioned within the nerve for 6 hours. In the second subject (C91) the NASA1 single-shank probe was inserted into a total of seven different sites. In each case, the electrode was inserted in planes judged to be parallel to the nerve axis. On average, the electrode was allowed to dwell at each site for 60 minutes.

The histological assessment of insertion trauma was conducted using light-level inspection of 1.5 micron thick whole-nerve sections. The results of surveys from two animals indicate cases of both significant trauma and undetectable levels of damage. Figure 16 shows photomicrographs from these two subjects. In the case of the 6 hour PSU4 insertion (Figure 16-A), there is evidence of a large region of trauma consistent with the electrode entry point and insertion angle. This region is characterized by a void following the insertion track and cellular debris within the void. Within this void are numerous instances of axons with disrupted membranes (Figure 16-C) that were not observed at any other locations within the nerve sections. The large region of trauma observed in subject C86 contrasted with the results from subject C91, in which we were unable to visually detect any signs of insertion trauma across all tissue samples.

There are two likely reasons for the markedly greater damage observed with the PSU4 insertion. First, that electrode was inserted for a relatively long time period. Differential motion of the probe and nerve over the 6 hr period could have aggravated the tissue damage due to the insertion trauma. Also, the PSU4 electrode was inserted in a plane orthogonal to the nerve axis. These results indicate that it is possible to insert thin-film electrodes into the cat auditory nerve with minimal damage as assessed by light microscopy. However, the results also show that these probes can cause damage that may be related to the duration of insertion or the dimensions and orientation of the probe. With our limited assessment, we are unable to determine the precise causal factors that led to the damage with the PSU4 electrode. However, it provides a cautionary note for future efforts.

Recordings of acoustically evoked response

Figure 17 show typical responses recorded from a single-shank PSU4 electrode array. Responses were recorded from 6 thin-film electrodes as well as from an electrode positioned on the round window

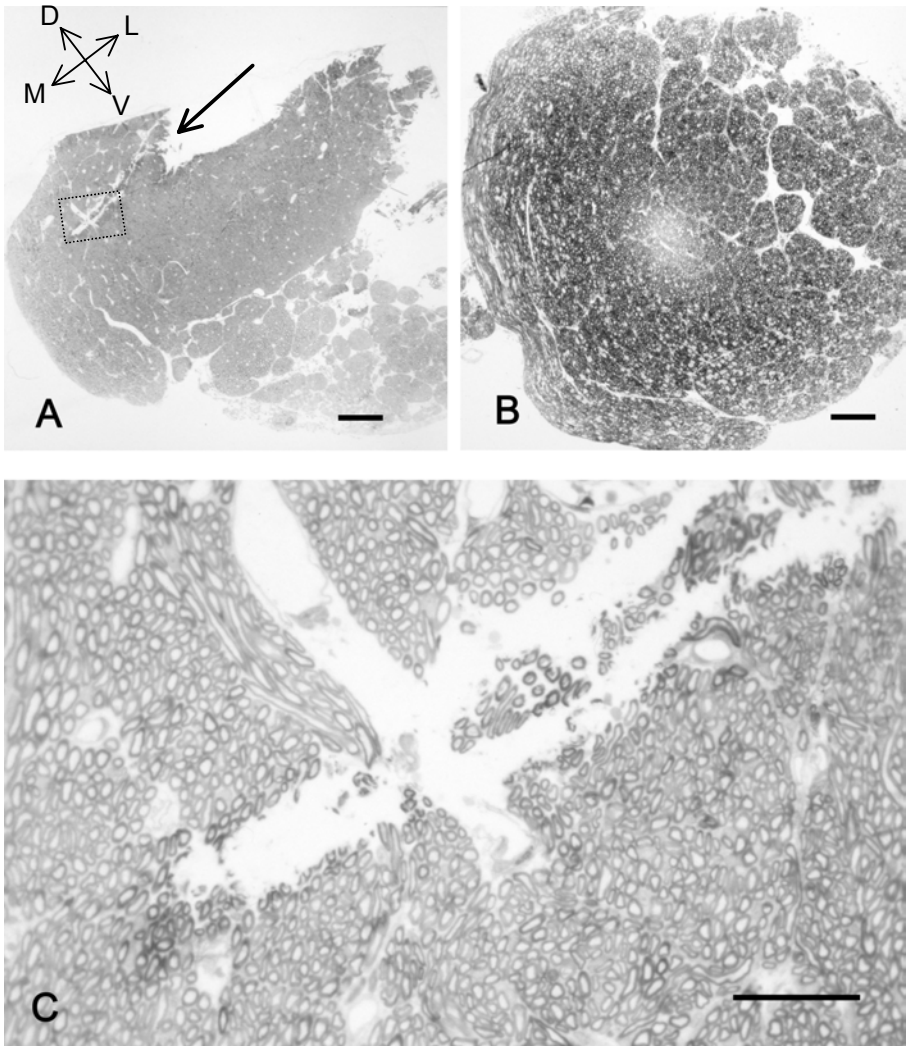

Figure 16 Photomicrographs of auditory nerve trunk cross-sections taken from preserved tissue dissected from two feline subjects at the conclusion of physiological experiments with CNCT thin-film electrodes. Sections were chosen to show significant insertion trauma in the case of subject C86 (panels A and C) and no detectable trauma in the second case of subject C91 (B). Orientation compass in panel A indicates dorsal-ventral and medial-lateral axes. Single arrow in panel A indicates insertion vector for the PSU4 electrode. Region of trauma (stippled box in panel A) is shown in the higher-power photograph of panel C. Calibration bars: A: 0.25 mm, B: 0.1 mm, C: 0.05 mm.

membrane. Response waveforms are plotted in response to four stimulus frequencies. The responses of the electrodes are relatively broad across the range of stimulus frequencies. Nevertheless the largest response is evident on a different electrode for each stimulus frequency, suggesting some degree of spatial selectivity. In addition, the spatial selectivity could possibly be improved if one takes into account differences in waveform across electrodes, as is evident in the strong phase reversal between electrodes 5 and 7 for 4100-Hz stimulation.

While the response amplitudes across electrodes generally demonstrate relatively broad spatial spread, in some conditions we have observed highly specific responses on a particular electrode. An example is shown in Figure 18. That figure shows responses from a PSU4 electrode with 8 intraneural contacts. The responses shown were obtained in response to a 1 kHz tone burst at levels of 34, 44 and 54 dB SPL. The responses are similar across contacts at the lowest stimulus level; however, a large response peak limited to electrode 5 emerges at higher stimulus levels. This example of highly restricted spatial response was, however, unusual in our experience with these electrodes.

In many cases we have used tuning curves, or iso-response functions, to characterize the frequency tuning at each electrode location. Response amplitude is simply determined by the amplitude variation within a fixed time window, thus ignoring any phase effects as illustrated in Figure 17. Examples of tuning curves shown in Figure 19 are typical of our recordings. In this case we used a 3-shank electrode array. The plots of the figure show the level needed to evoke a 30-μV criterion response amplitude as a function of stimulus frequency. While there are some differences in tuning, particularly for electrodes 1, 5 and 6, most electrodes show similar frequency selectivity.

The data such as those shown in Figures 17-19 must be put in the perspective of the rather complex tonotopic organization of the auditory nerve (Sando, 1965). While there is some evidence of spatial selectivity in the data collected with the thin-film electrodes thus far, on the whole, the frequency response functions for different electrodes do not show the specificity that would likely be necessary to develop a clear frequency map. Future efforts could be directed toward improving the likelihood of obtaining spatially specific responses. For example, pairs of recording electrodes could be used to obtain differential potentials (possibly at the cost of more complex interpretation). Such differential electrode recordings would optimally be made using electrode contacts designed specifically for this task. Also, by using the second spatial derivative of the voltage distributions, a "current source density" analysis could be used to better extract spatial information.

Recordings of electrically evoked responses to assess conduction velocity

We also used the 3-shank probe to measure conduction velocity in the auditory nerve. In those experiments, the electrode array was inserted into the nerve so that the three shanks of the electrode lined up longitudinally along the length of the nerve trunk. In that way we could take advantage of the fixed distance between the shanks and compare response latency between electrodes on adjacent shanks to assess conduction velocity. In order to produce highly synchronized responses we used electrical stimulation using a intracochlear electrode array. Typical responses recorded from 3 electrodes, each on a different shank of the thin-film electrode array, are shown in Figure 20. The latency of the N1 peak was measured for each electrode in the array and plotted in Figure 21-A. The recordings from electrodes in the same row, i.e., the same height in the array are connected. In general, the electrodes in more distal locations result in a shorter latency response. By comparing latency from different shanks, the conduction velocity can be calculated and plotted in Figure 21-B. While there are some variations in the estimated conduction velocity, these initial results suggest a conduction velocity on the order of 10-13 m/s. We note however, that these estimates were obtained at a lowered nerve temperature (approximately 36° C) due to surgical exposure. Using a controlled temperature saline wash, we have observed a strong dependence (approximately 1 m/s/°C) on temperature.

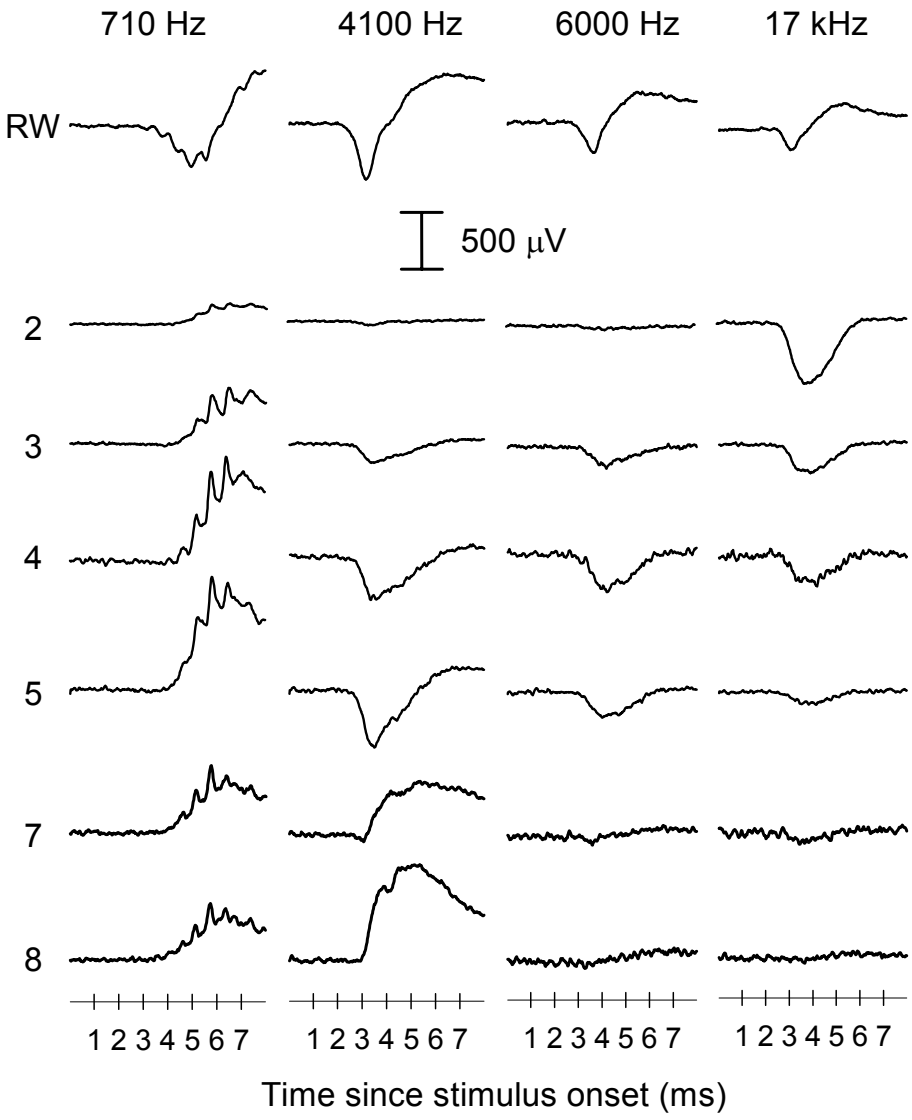

Figure 17 Examples of tone-burst evoked potentials recorded by a PSU4 thin-film electrode array inserted into the nerve trunk of subject C86. Each column depicts the responses obtained from six of the eight PSU4 electrodes (i.e., rows labeled 2 through 8) plus an extracochlear electrode positioned on the round window (top row, labeled "RW"). Responses to a different stimulus frequency are shown in each of the four columns. In each case, the stimulus levels were chosen to be between 30 and 50 dB of the visual detection threshold for the round window electrode. Note the phase-locked responses for the lowest stimulus frequency and the reversal of waveform polarity across recording sites for the case of the 4.1 kHz tone burst. All waveforms are plotted to the same scales.

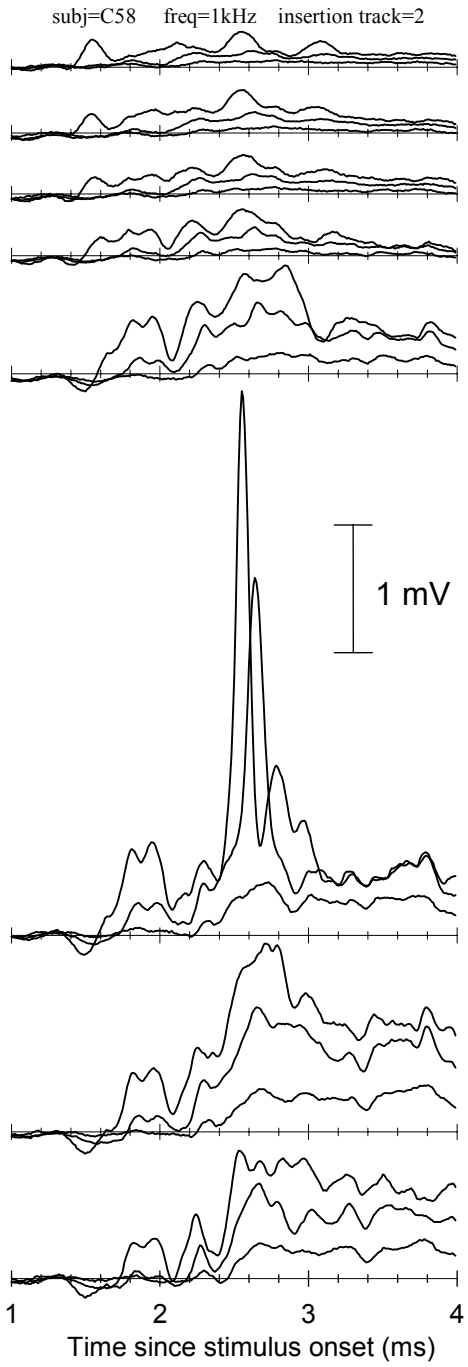

Figure 18 Additional examples of evoked response waveforms recorded using a PSU4 thin-film probe inserted into the nerve trunk of subject C58. Shown in each of the eight panels are waveforms evoked using a 1 kHz tone burst at sound levels of 34, 44, and 54 dB SPL. All waveforms exhibit what could be described as a common-mode response, that is, temporal response patterns highly correlated across electrodes. However, the sixth electrode exhibited a unique, high-amplitude response at the higher stimulus levels. Such an instance of a highly restricted spatial response pattern was a rare occurrence in our feasibility study of using thin-film electrodes in the auditory nerve. All waveforms are plotted to the same scales.

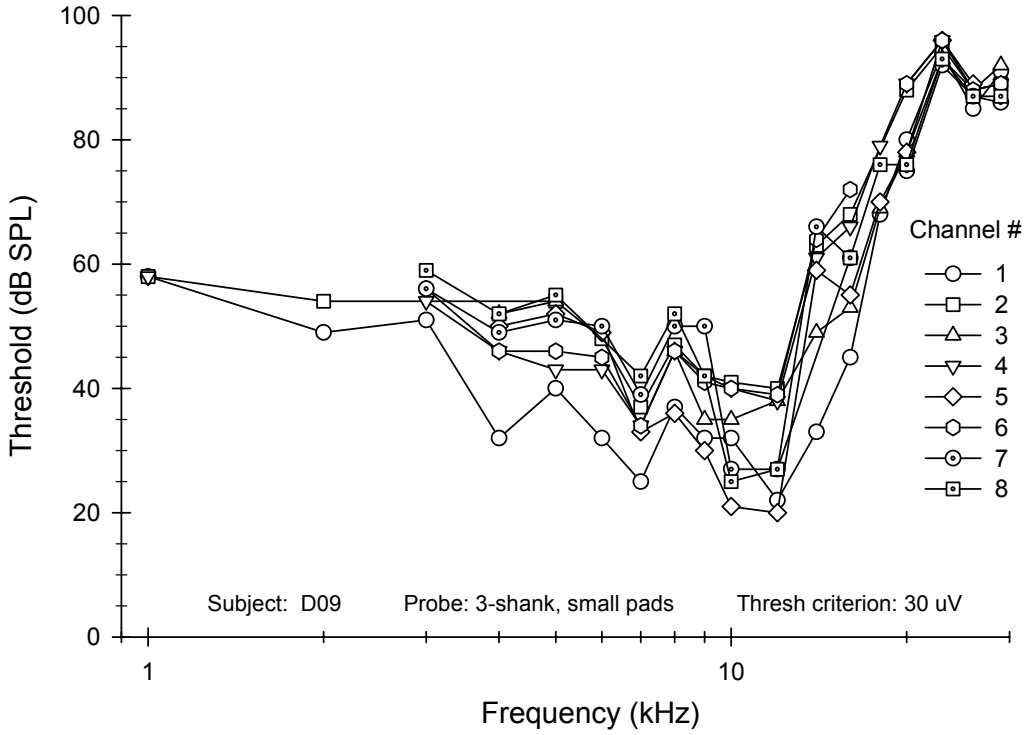

Figure 19 Tuning curves for evoked potentials recorded by 8 electrodes of a three-shank thin-film array (cf Figure 15-C) inserted into the cat auditory nerve trunk. The 8 electrodes were chosen to sample each of the three shanks. Thresholds are plotted as the level necessary to elicit a criterion 30 μV response as a function of stimulus frequency.

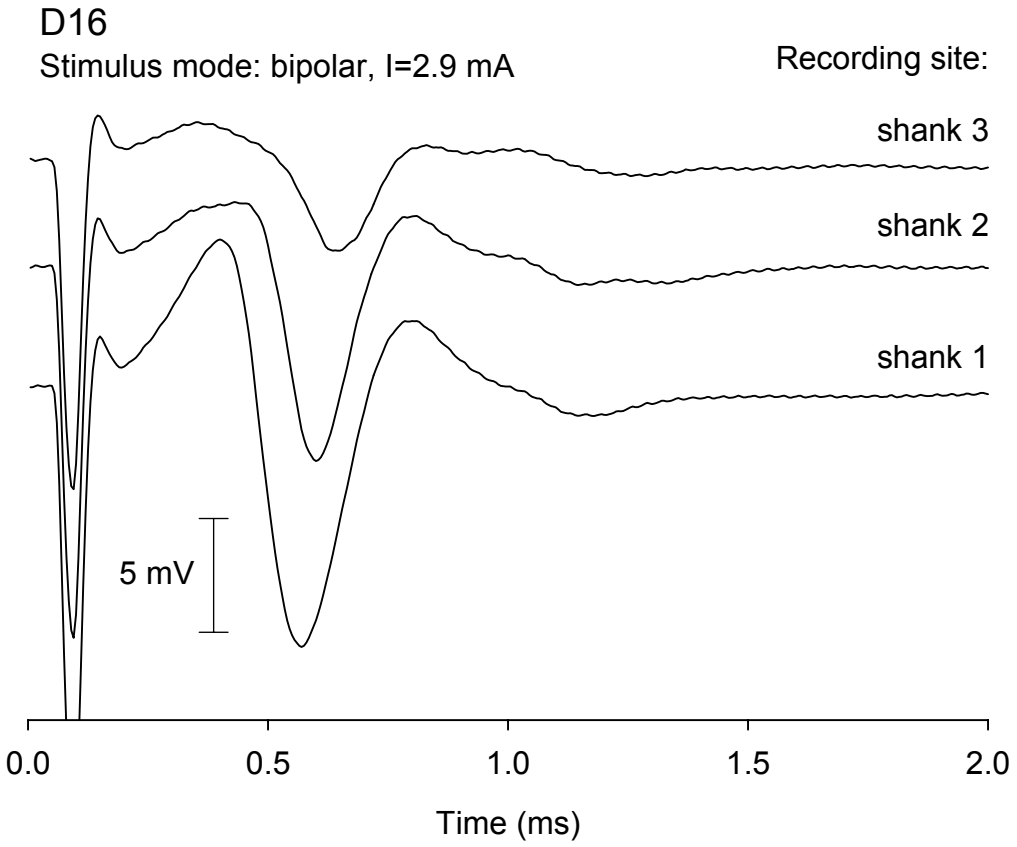

Figure 20 Responses recorded from electrodes on three different shanks of the three-shank auditory nerve-trunk probe in response to a single 40 us/phase current pulse. The probe was inserted into a plane approximately parallel to the axis of the nerve trunk. Shank 1 was positioned at the most peripheral site, while shank 3 was in the most centrally located site. Clear differences in response latency are evident, demonstrating that the thin-film electrodes can be used to obtain spatially specific responses within the auditory nerve.

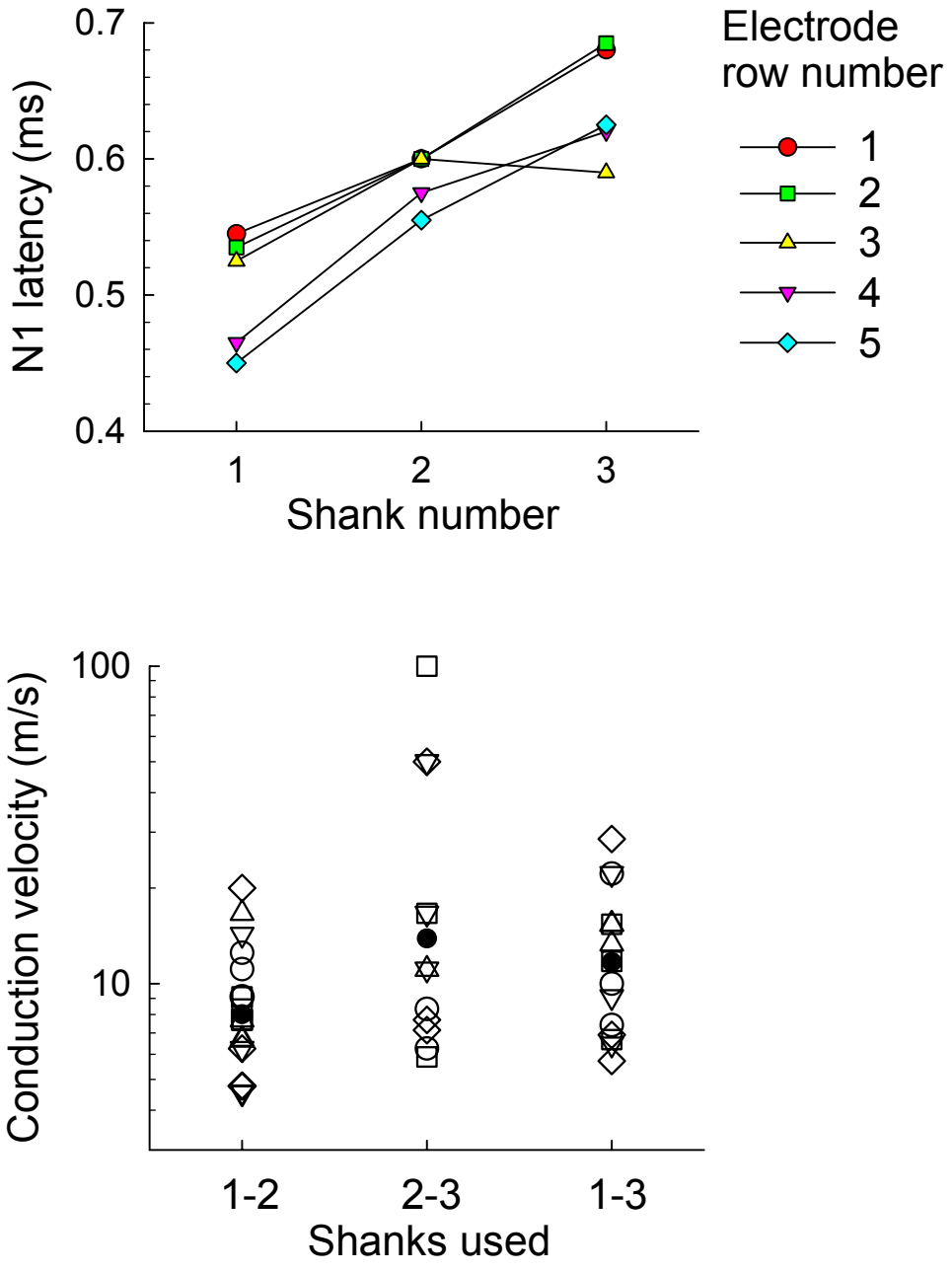

Figure 21 Panel A: Upper graph plots the latency of the N1 peak as a function of electrode shank number. The electrode was placed in the nerve so that shank 1 was the most distal. Recordings were made from 5 electrodes on each shank. Responses from electrodes in the same row are connected. Panel B: Calculated conduction velocity is plotted for each pairing of the three electrode shanks. Mean values are plotted with filled symbols. Data were collected with an estimated nerve trunk temperature of 36° C.

Accurate estimates of conduction velocity will assist in the development of appropriate computational models of the nerve. Furthermore, the issue of its temperature dependence, which has yet to be adequately addressed, is an important problem, particularly given its relevance to various temporal operties of nerve fibers and published speculation on mechanisms of spike conduction failure.

X. Peer-reviewed publications resulting from this contract work

Mino H., Rubinstein J.T., Miller C.A., Abbas P.A. (in press) Effects of electrode-to-fiber distance on temporal jitter with electrical stimulation. IEEE Trans. Biomed. Eng.

Abbas P.J., Miller C.A. (in press) Biophysics and Physiology. In Cochlear Implants, (eds F-G. Zeng, R. Fay and A. Popper) Springer-Verlag.

Hong R.S., Rubinstein J.T., Wehner D., Horn D. (2003). Dynamic range enhancement for cochlear implants. Otology & Neurotology. 24, 590-5.

Miller C.M., Abbas P.J., Nourski K.V., Hu N., Robinson B.K. (2003). Electrode configuration influences action potential initiation site and ensemble stochastic response properties. Hear. Res. 175, 200-14.

Rubinstein J.T. and Santina C.C.D. (2002). Development of a biophysical model for vestibular prosthesis research. J. Vestibular Res., 12, 69-76.

Matsuoka A.J., Rubinstein J.T., Abbas P.J., Miller C.A. (2001). The effects of interpulse interval on stochastic properties of electrical stimulation: Modes and measurements. IEEE Trans. Biomed. Eng. 48, 416-424.

Miller C.A., Abbas P.A., Robinson B.K. (2001). Response properties of the refractory auditory nerve fiber. JARO, 2, 216-232.

Miller C.M., Robinson B.K., Rubinstein J.T., Abbas P.J., Samuelson C.R. (2001). Auditory nerve responses to monophasic and biphasic electric stimuli. Hear. Res. 151, 79-99.

Rubinstein J.T., Miller C.A., Mino H., Abbas P.J. (2001). Analysis of monophasic and biphasic electrical stimulation of nerve. IEEE Trans Biomed. Eng. 48, 1065-1070.

Miller C.M., Abbas P.J., Brown, C.J. (2000) A new method of reducing stimulus artifact in the electrically evoked whole nerve potential. Ear Hear. 21, 280-290.

Matsuoka A.J., Abbas P.J., Rubinstein J.T., Miller, C.A. (2000a). The neuronal response to electrical constant-amplitude pulse train stimulation: Evoked compound action potential recordings. Hear. Res. 149, 115-128.

Matsuoka A.J., Abbas P.J., Miller C.A., Rubinstein J.T. (2000b). The neuronal response to electrical constant-amplitude pulse train stimulation: additive gaussian noise. Hear. Res. 149, 129-137.

REFERENCES

Abbas P.J., Matsuoka A.J., McDougal V.M., Miller C.A., Rubinstein J.T. (1998). Compound action potential responseto electrical amplitude-modulated pulse trains in the guinea pig auditory nerve. Abstr. ARO Midwinter Meeting.

Abbas P.J., Brown C.J. (2000). Electrophysiology and device telemetry. In S. Waltzman & N. Cohen (Eds.) Cochlear Implants, (pp. 117-150). New York: Thieme.

Abbas P.J., Hughes M.L., Brown C.J., Miller C.A. (2002). Electrophysiological assessment of stimulation selectivity. Candidacy for implantable hearing devices, Utrecht, The Netherlands.

Abbas P.J., Brown C.J., Hughes M.L., Etler C.P., Behrens A., Dunn S.M. (2003). The electrically evoked compound action potential: channel interaction measures. Conference on Implantable Auditory Prostheses, Pacific Grove, CA.

Abkes B.A., Miller C.A., Hu N., Abbas P.J. (2003). Adaptation in the auditory nerve in response a continuous electric pulse train. ARO Midwinter Meeting.

Arenberg J.G., Furukawa S., Middlebrooks J.C. (2000) Auditory cortical images of tones and noise bands. JARO 1, 183-94.

Arenberg Bierer J., Snyder R.L., Middlebrooks J.C. (2002) Temporal Response Properties of Inferior Colliculus Neurons for Acoustical and Electrical Cochlear Stimulation. Assoc. Res. Otolaryngol. Abs., Abstract 541.

Berry K.J. & Meister M. (1998). Refractoriness and neural precision. J. Neurosc., 18, 2200-2211.

Brown C.J., Abbas P.J. (1990). Electrically evoked whole-nerve action potentials: parametric data from the cat. J Acoust Soc Am 88, 2205-10.

Brown C.J. Abbas P.J., Gantz B. (1990). Electrically evoked whole-nerve action potentials: data from human cochlear implant users. J Acoust Soc Am 88, 1385-91.

Brown C.J., Hughes M.L., Lopez S.M., & Abbas P.J. (1999). The relationship between EABR thresholds and levels used to program the Clarion speech processor. Annals of Otology Rhinology and Otolaryngology, 108, Suppl. 177, 50-57.

Busby P.A., Tong Y.C., Clark G.M. (1993). The perception of temporal modulations by cochlear implant patients. Journal of the Acoustical Society of America. 94,124-31.

Charasse B., Thai-Van H., Berger-Vachon, C., Collet L. (2003). Assessing auditory nerve recovery function with a modified subtraction method: results and mathematical modeling. Clinical Neurophysiology, 114, 1307-15.

Cohen L.T., Knight M.R., Saunders E., & Cowan R.S.C. (2001). Characteristics of NRT measurement in CI24 Nucleus contour electrode and straight arrays. (Abstract) Conference on Implantable Auditory Prostheses, Pacific Grove, CA.

Dolphin W.F. & Mountain D.C. (1992). The envelope following response: scalp potentials elicitedinthe Mongolian gerbil using sinusoidally AM acoustic signals. Hear. Res., 58, 70-78.

Finley C.C., Wilson B., van den Honert C., & Lawson D. (1997). Speech Processors for Auditory Prostheses. *Sixth Quarterly Progress Report*, NIH Contract NO1-DC-5-2103.

Galambos R., Makeig S., & Talmachoff P.J. (1981). A 40-Hz auditory potential recorded from the human scalp. Proc. Natl. Acad. Sci., 78, 2643-47.

Haenggeli A., Zhang J.S., Vischer M.W., Pelizzone M., & Rouiller E.M. (1998). Electrically evoked compound action potential (ECAP) of the cochlear nerve in response to pulsatile electrical stimulation of the cochlea in the rat: Effects of stimulation at high rates. Audiology, 37(6), 353-71.

Hong R.S., Rubinstein J.T., Wehner D., Horn D. (2003). Dynamic range enhancement for cochlear implants. Otology & Neurotology. 24, 590-5.

Jeng F.-C., Abbas P.J., Brown C.J., Miller C.A., Robinson B.K., Nourski K.V. (2003). Electrically evoked steady-state responses. Conference on Implantable Auditory Prostheses, Pacific Grove, CA.

Killian M.J.P., Klis S.F.L., & Smoorenburg G.F. (1994). Adaptation in the compound action potential response of the guinea pig VIIIth nerve to electric stimulation. Hear. Res., 81, 66-82. n

Kuwada S., Batra R. & Maher V.L. (1986). Scalp potentials of normal and hearing impaired subjects in response to sinusoidally amplitude-modulated tones. Hear. Res., 21, 179-192.

Liang D.H., Lusted H.S., White R.L. (1999). The nerve-electrode interface of the cochlear implant: current spread. IEEE Trans Biomed Eng 46, 35-43.

Litvak L. (2002). Towards a better speech processor for cochlear implants: Auditory-nerve responses to high-rate electric pulse trains. MIT Doctoral Thesis.

Litvak L., Delgutte B., & Eddington D. (2001). Auditory nerve fiber responses to electric stimulation: modulated and unmodulated pulse trains. J. Acoust. Soc. Am., 110, 368-79.

Matsuoka A.J., Rubinstein J.T., Abbas P.J., & Miller C.A. (2001). The effects of interpulse interval on stochastic properties of electrical stimulation: Modes and measurements. Trans. on Biomed. Eng., 48, 416-424.

Matsuoka A.J., Abbas P.J., Rubinstein J.T., & Miller C.A. (2000). The neuronal response to electrical constant-amplitude pulse train stimulation: Evoked compound action potential recordings. Hearing Research, 149, 115-128.

Matsuoka A.J., Abbas P.J., Miller C.A., & Rubinstein J.T. (2000). The neuronal response to electrical constant-amplitude pulse train stimulation: Additive Gaussian noise. Hearing Research, 149, 129-137.

Meyer T.T., Rubinstein J.T., Hong, R. (2003) Effects of High-Rate Pulse Trains on Frequency Discrimination by Cochlear Implant Users. ARO Midwinter Meeting.

Miller C.A., Abbas P.J., Rubinstein J.T., Robinson B.K., Matsuoka A.J. (1997). Quarterly progress report # 6, The Neurophysiological Effects of Simulated Auditory Prosthesis Stimulation, NIH contract NO1-DC-6-2111

Miller C.A., Abbas P.J., Rubinstein J.T., Robinson B.K., Matsuoka A.J., & Woodworth, G. (1998). Electrically evoked compound action potentials of guinea pig and cat: Response to monopolar, monophasic stimulation. Hear. Res., 119, 142-154.

Miller C.A., Abbas P.J., Robinson B.K., Rubinstein J.T., & Matsuoka, A.J. (1999a). Electrically evoked single-fiber action potentials from cat: Responses to monopolar, monophasic stimulation. Hear. Res., 130, 197-218.

Miller C.A., Abbas P.J., & Rubinstein, J.T. (1999b). An empirically based model of the electrically evoked compound action potential. Hear. Res., 135, 1-18.

Miller C.A., Abbas P.J., Brown C.J. (2000) An improved method of reducing stimulus artifact in the electrically evoked whole nerve potential, Ear & Hear. 21, 280-290.

Miller C.A., Abbas P.J., & Brown C.J. (2001a). Physiological measurements of spatial excitation patterns produced by electrical stimulation (Abstr.). Conference on Implantable Auditory Prostheses, Pacific Grove, CA.

Miller C.A., Abbas P.J., & Robinson, B.K. (2001b). Response properties of the refractory auditory nerve fiber. JARO, 2, 216-232.

Miller C.A., Robinson, B.K., Rubinstein, J.T., Abbas, P.J., & Runge-Samuelson, C. (2001c) Auditory nerve responses to monophasic and biphasic electric stimuli Hear. Res. 151, 79-94.

Miller C.A. Abbas, P.J. Nourski, K.V. Hu, N. Robinson, B.K. (2003). Electrode configuration influences action potential initiation site and ensemble stochastic response properties. Hearing Research, 175, 200-14.

Mino H., Rubinstein, J.T., Miller C.A., Abbas P.A. (in press) Effects of Electrode-to-Fiber Distance on Temporal Jitter with Electrical Stimulation. IEEE-TBME.

Mino H., Rubinstein, J.T. and White, J.A. (2002). Comparison of computational algorithms for the simulation of action potentials with stochastic sodium channels. Annals of Biomendical Engineering, 30, 578-587.

Pfingst B.E., Zwolan T.A., & Holloway L.A. (1997). Effects of stimulus configuration on psychophysical operating levels and on speech recognition with cochlear implants. Hear. Res., 112, 247-260.

Pfingst B.E., Franck K.H., Xu L., Bauer E.M., & Zwolan T.A. (2001). Effects of electrode configuration and place of stimulation on speech perception with cochlear prostheses. JARO, 2, 87-103.

Rubinstein J.T. (1988). Quasi-static analytical model for electrical stimulation of the auditory nervous system. Doctoral Dissertation, University of Washington, Seattle, WA.

Rubinstein J.T. (1995). Threshold fluctuations in an N Sodium Channel Model of the Node of Ranvier. Biophysical J., 68, 779-785.

Rubinstein J.T. and Santina C.C.D. (2002). Development of a biophysical model for vestibular prosthesis research. J. Vestibular Res., 12, 69-76.

Rubinstein J.T., Wilson B.S., Finley C.C., & Abbas P.J. (1999). Pseudospontaneous activity: Stochastic independence of auditory nerve fibers with electrical stimulation. Hear. Res., 127, 108-118.

Rubinstein J.T., Miller C.A. Mino H., & Abbas P.J. (2001). Analysis of Monophasic and biphasic electrical stimulation of nerve. IEEE Trans BME, 48, 1065-1070.

Rubinstein J.T., Tyler R.S., Johnson A., Brown C.J. (2003). Electrical suppression of tinnitus with high-rate pulse trains. Otology & Neurotology. 24, 478-85.

Runge-Samuelson C.L., Rubinstein J.T., Abbas P.J., Miller C.A., Smith G.J., Robinson B.K., & Abkes B.A. (2001a). Sinusoidal electrical stimulation of the auditory nerve with and without high-rate pulses. (Abstract) Conference on Implantable Auditory Prostheses, Pacific Grove, CA.

Runge-Samuelson C.L., Rubinstein J.T., Abbas P.J., Miller C.A., Smith G.J., Robinson B.K., & Abkes B.A. (2001b). Sinusoidal electrical stimulation of the auditory nerve with and without high-rate pulses. (Abstract) 24th Annual Midwinter Research Meeting, St. Petersburg Beach, FL.

Sando I. (1965). The anatomical interrelationships of the cochlear nerve fibers. Acta Otolaryngol. (Stockh.) 59, 417-435.

Shannon RV. (1992). Temporal modulation transfer functions in patients with cochlear implants. J. Acoust. Soc. Am. 91, 2156-64.

Shepherd R.K., Hatsushika S., Clark G.M. (1993). Electrical stimulation of the auditory nerve: the effect of electrode position on neural excitation. Hear. Res. 66, 108-20.

Shepherd R.K., & Javel E. (1997). Electrical stimulation of the auditory nerve. I. Correlation of physiological responses with cochlear status. Hear. Res. 108 , 112-144.

Shepherd R.K., & Javel E. (1999). Electrical stimulation of the auditory nerve: II. Effect of stimulus waveshape on single fibre response properties. Hear. Res. 130, 171-88.

Smith D.W., White M.W. (1995) The effect of changes in intracochlear electrode configuration on behavioral strength-duration curves for electrical stimuli in the cat. Assoc. Res. Otolaryngol. Abs., Abstract 708. p 177.

Snyder R., Bonham B., Rebscher S. (2003) Quarterly progress report #2 The Neurophysiological Effects of Simulated Auditory Prosthesis Stimulation. Contract N01-DC-02-1006.

Stypulkowski P.H., & van den Honert C. (1984). Physiological properties of the electrically stimulated auditory nerve. I. Compound action potential recordings. Hear. Res., 14, 225-243.

Verveen A.A. (1961). Fluctuation in Excitability, Drukkerjj Holland N.V., Amsterdam.

White M.W. (1984). Psychophysical and neurophysiological considerations in the design of a cochlear prosthesis. Audiol. Ital., 1, 77-117.

Wilson B.S., Finley C.C., Zerbi M., & Lawson, D. (1995). Speech Processors for Auditory Prosthesis, Eleventh Quarterly Progress Report, NIH Contract N01-2-2401, Center for Auditory Prosthesis Research.

Wilson B.S., Finley C.C., Lawson D.T., & Zerbi M. (1997). Temporal representations with cochlear implants. Am. J. Otol., 18, S30-34.

Xi X., Hong M., Ji F., Han D. & Yang W. (2003). Spatial pattern of neural excitation measured on electrode band of cochlear implant. Chinese Journal of Audiology, 1, 25-28.